# Supporting Informatiom

## Micelle-mediated Synthesis of Quinoxaline, 1,4-Benzoxazine and 1,4-Benzothiazine Scaffolds from Styrenes

**Bisma Teli,[†‡#] Mohmad Muzafar Wani,[†‡#] Shafia Jan, Haamid Rasool Bhat[†] and Bilal A. Bhat[†‡*]**

CSIR-Indian Institute of Integrative Medicine, Sanatnagar Srinagar-19005, India;
+91-1942431253;
‡Academy of Scientific and Innovative Research (AcSIR), Ghaziabad-201002, India
E-mail: bilal@iiim.res.in

# Equal contribution

## Contents

# $^{1}H$ and $^{13}C$ NMR of Compound **3a**

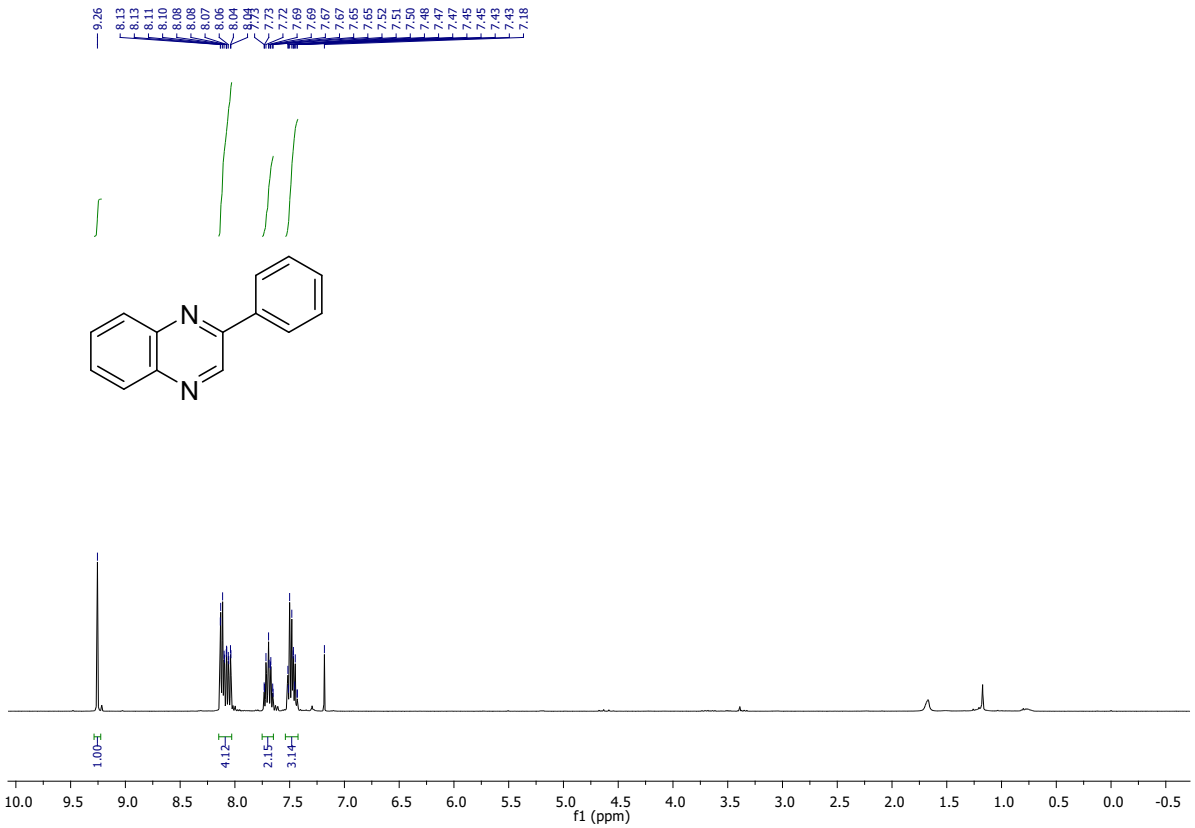


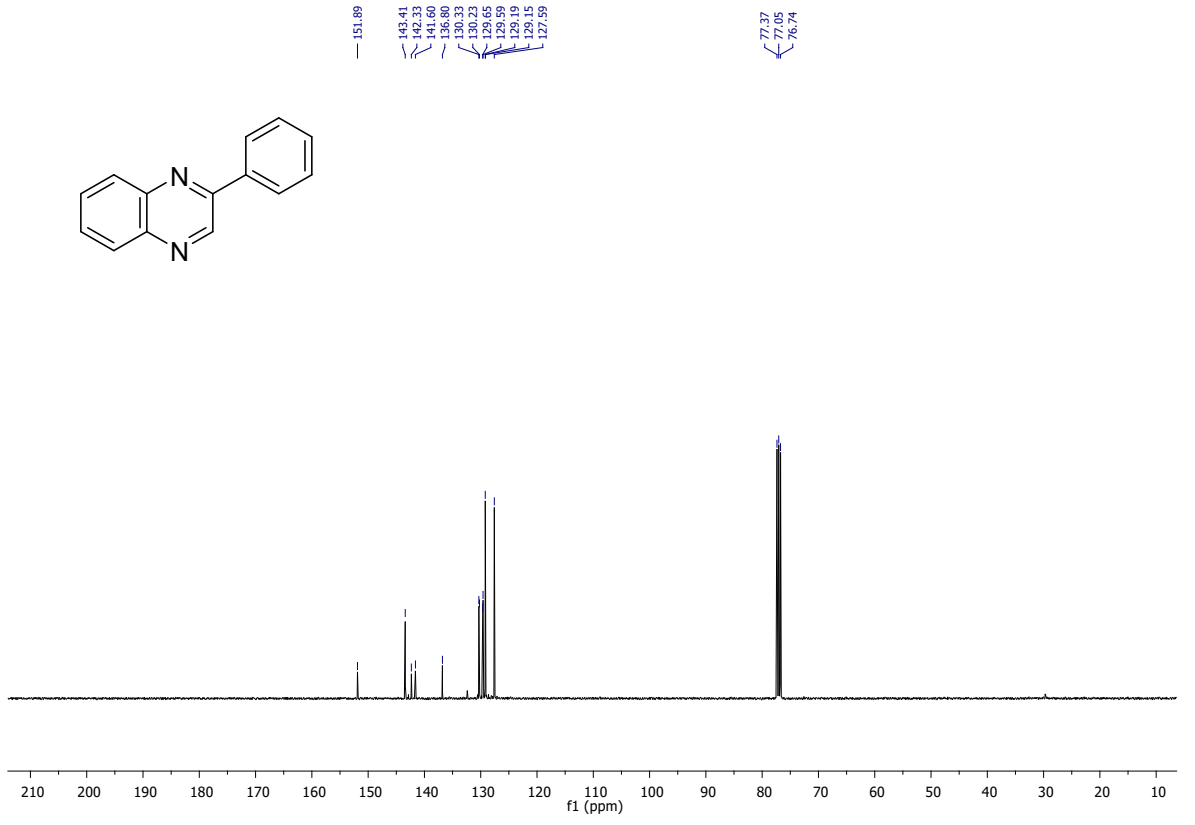

# $^{1}H$ and $^{13}C$ NMR of Compound **3b**

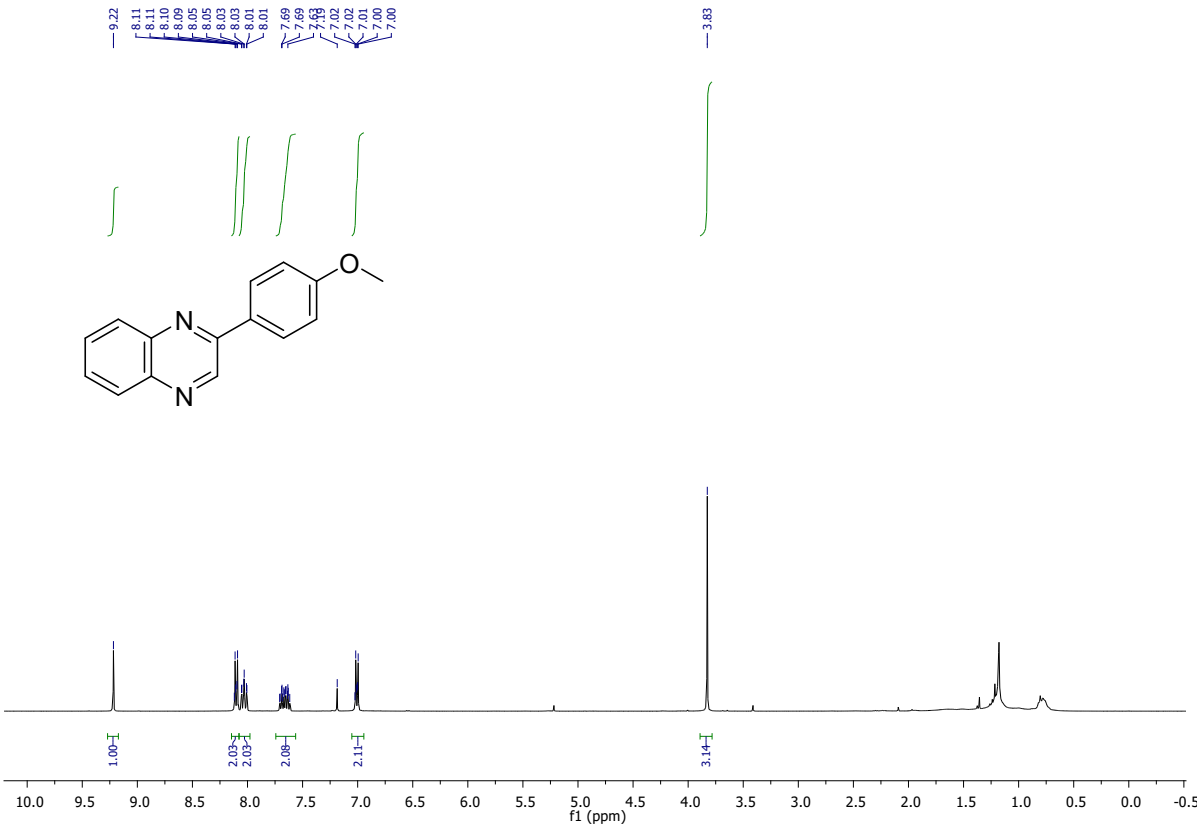


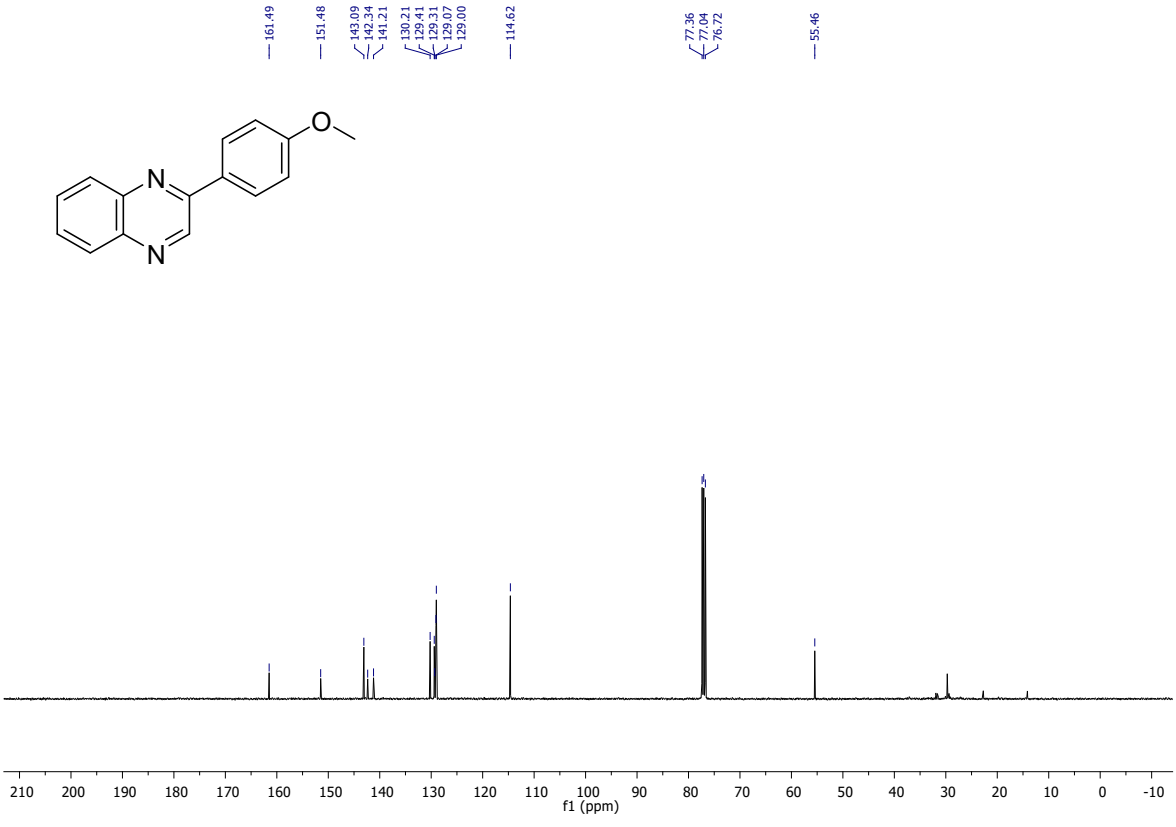

# $^{1}H$ and $^{13}C$ NMR of Compound **3c**

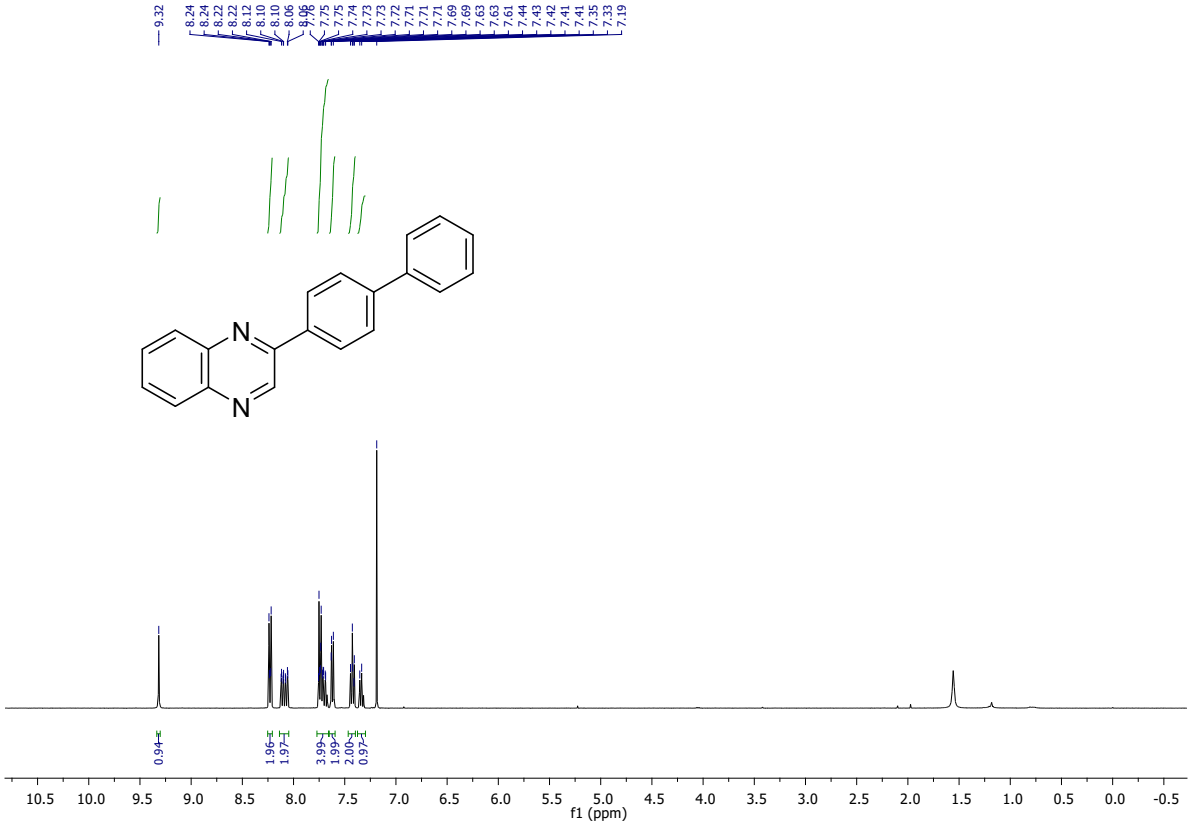


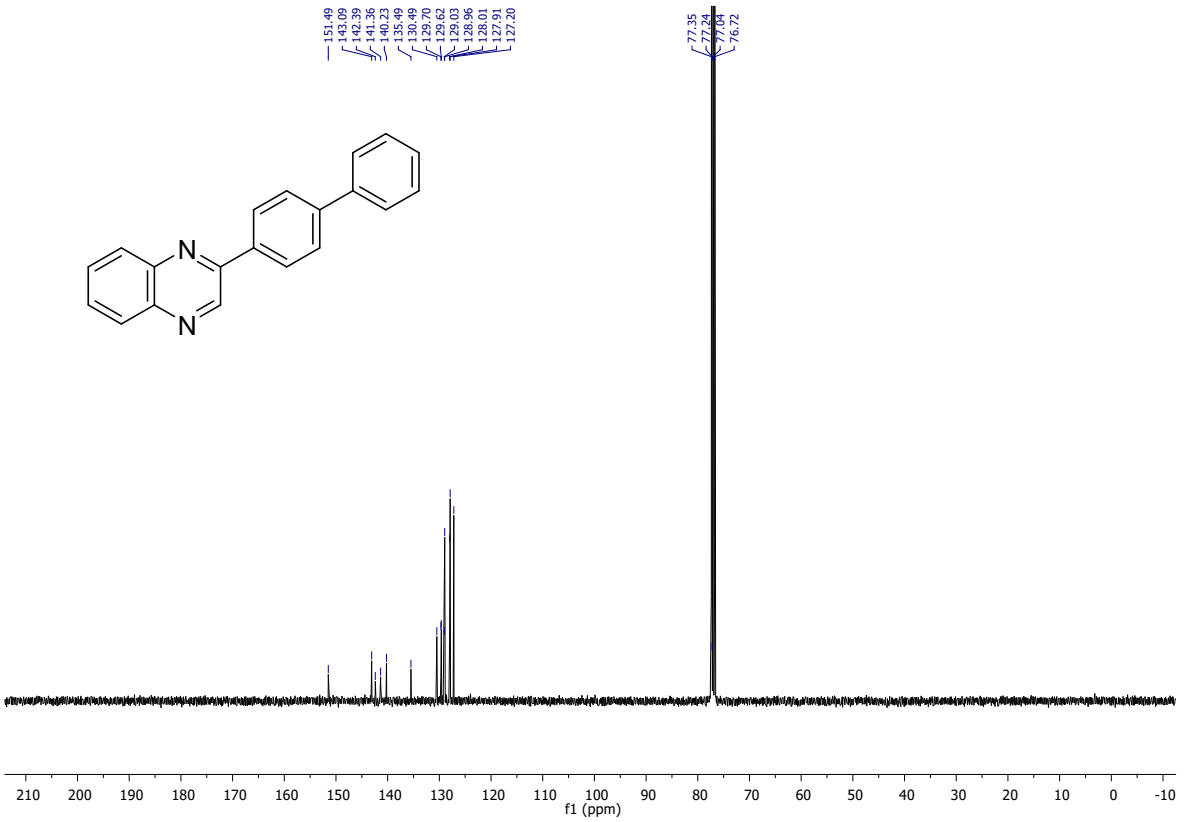

# $^{1}H$ and $^{13}C$ NMR of Compound **3d**

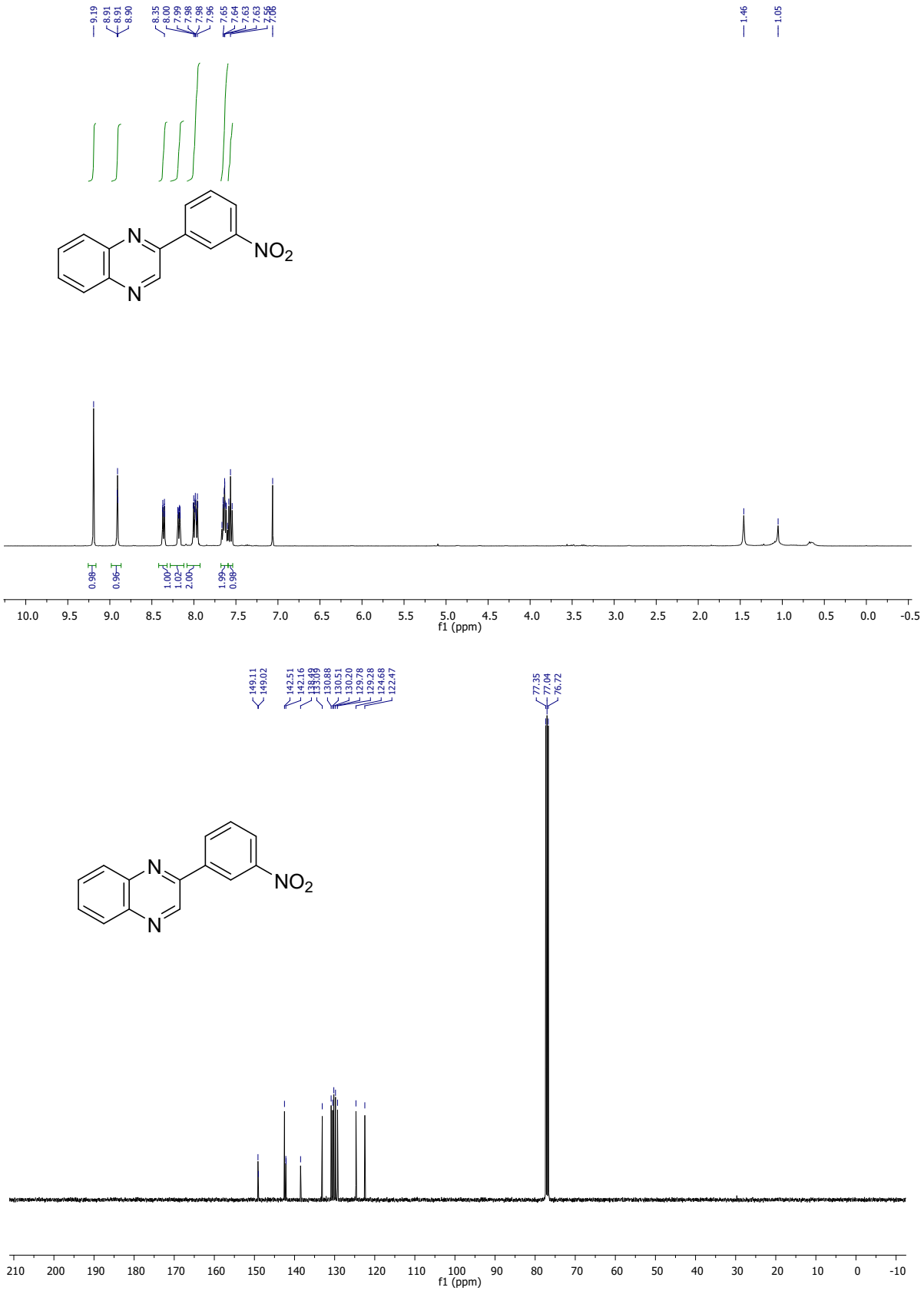

# $^{1}H$ and $^{13}C$ NMR of Compound **3e**

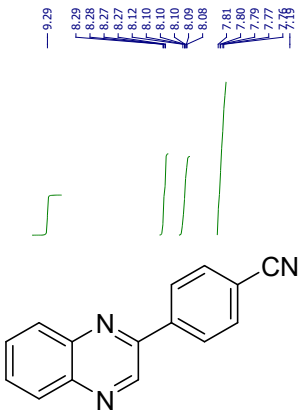


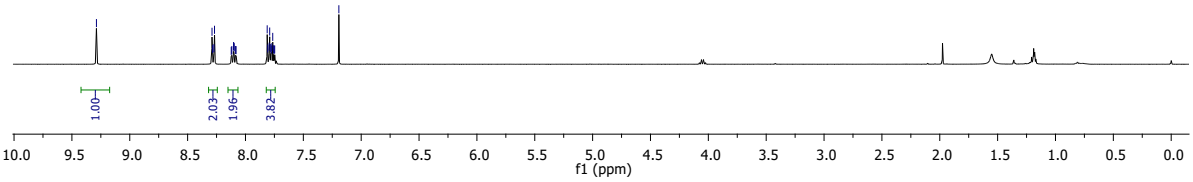



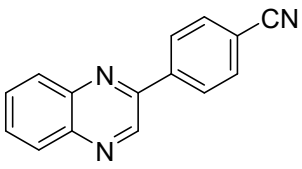


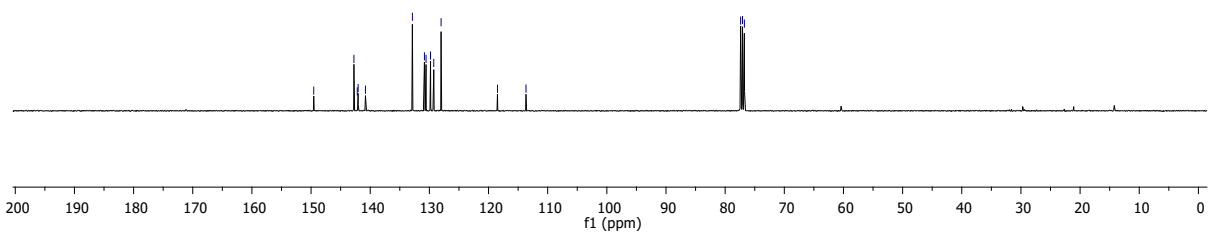

# $^{1}H$ and $^{13}C$ NMR of Compound **3f**

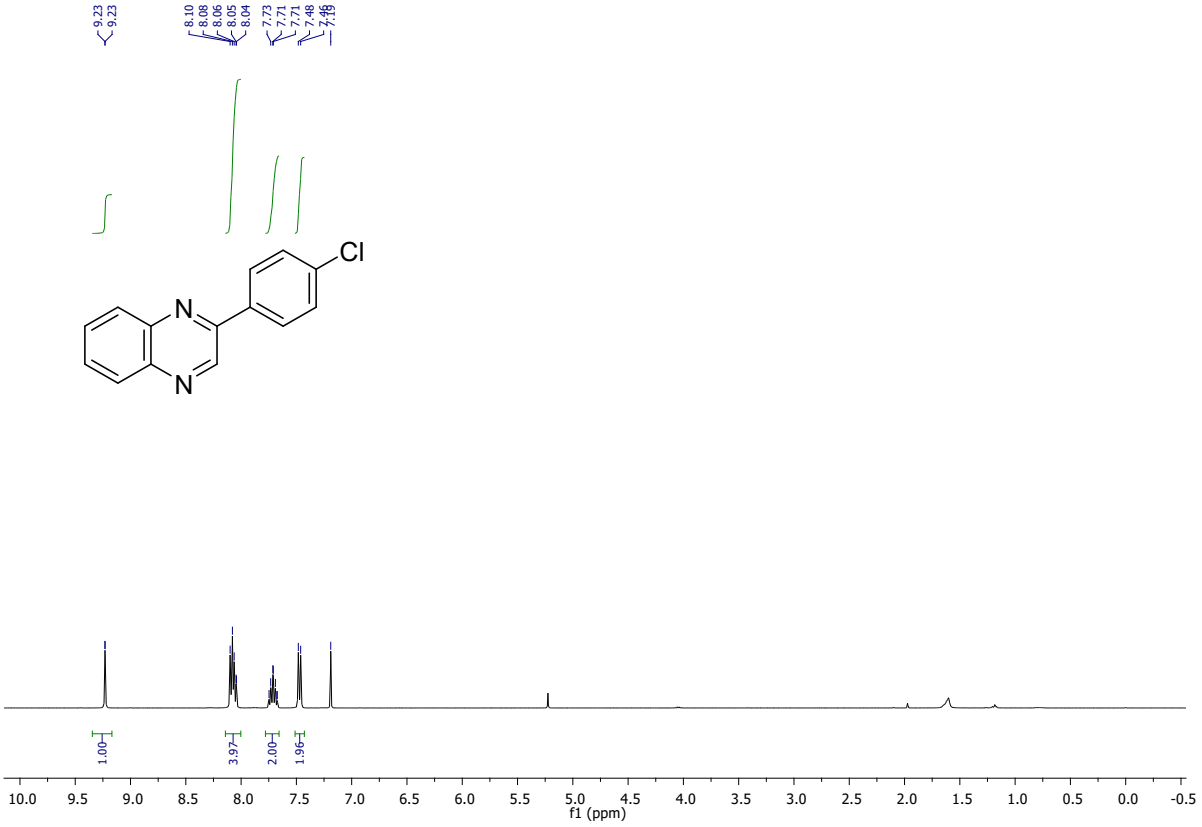


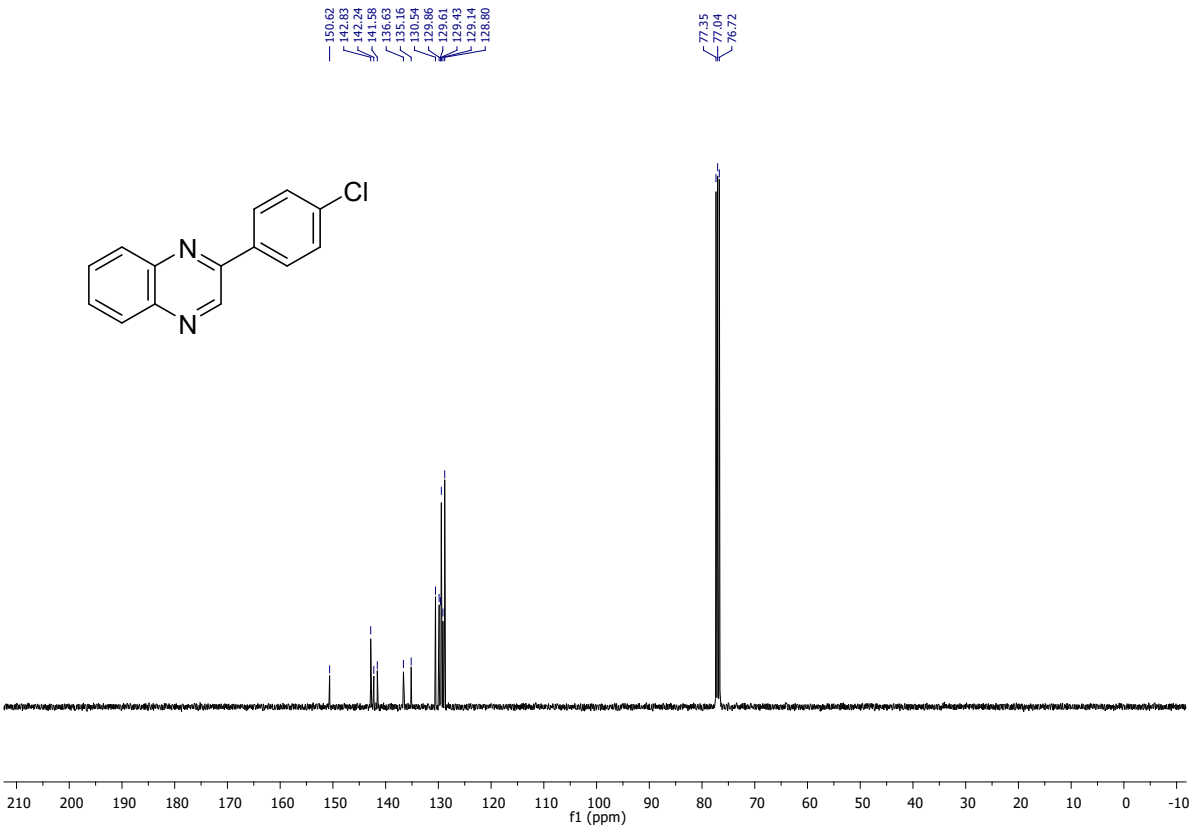

# $^{1}H$ and $^{13}C$ NMR of Compound **3g**

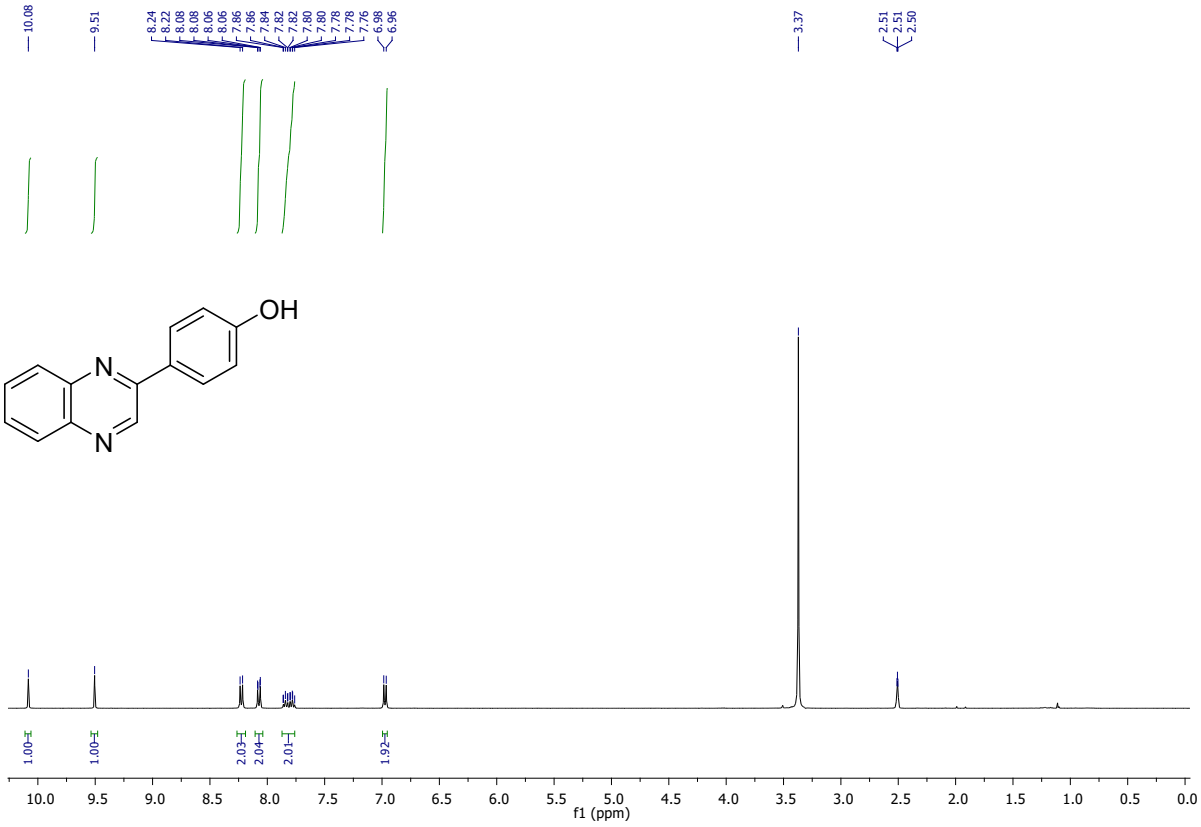


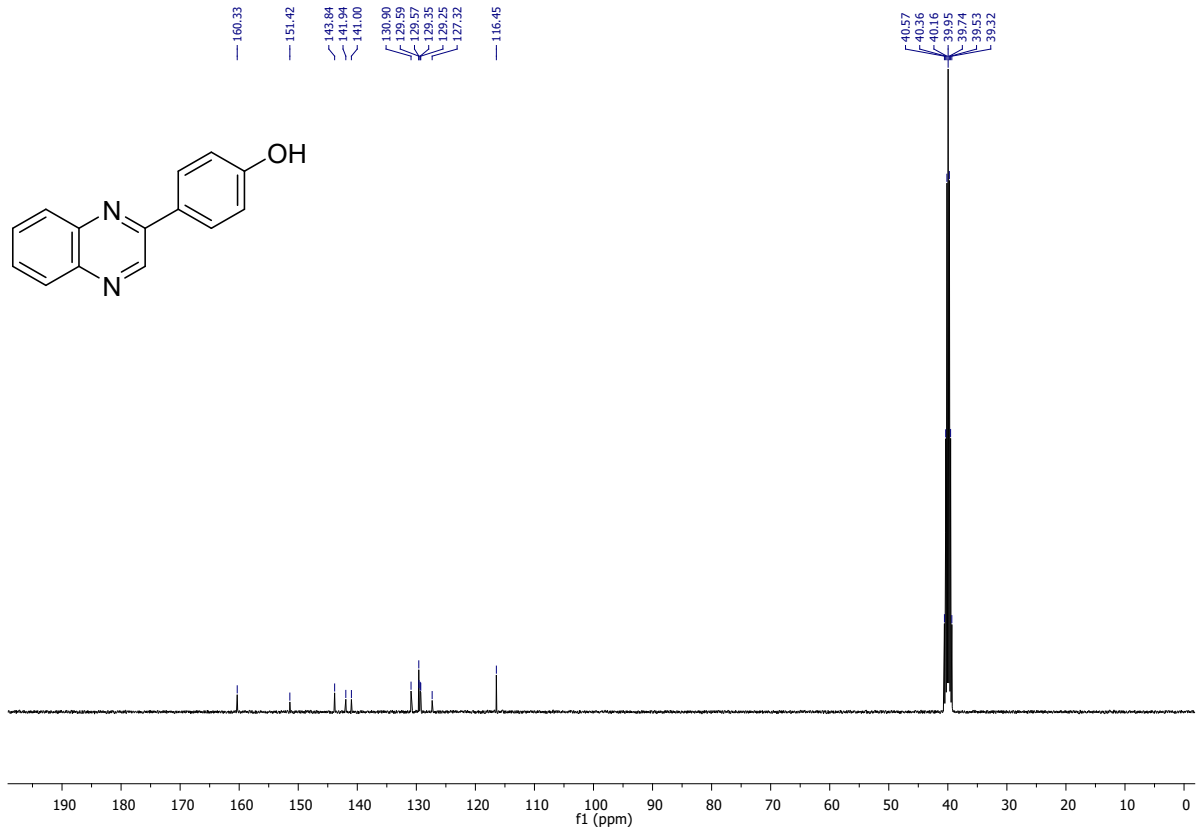

# $^{1}H$ and $^{13}C$ NMR of Compound **3h**

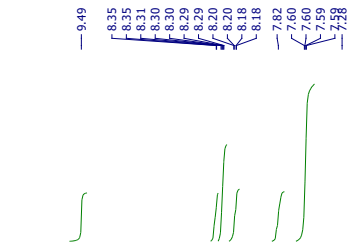


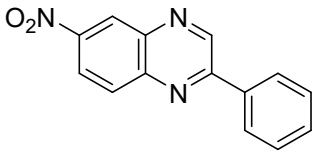


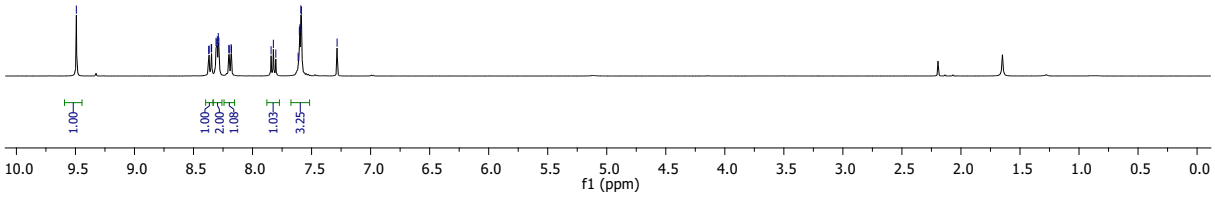



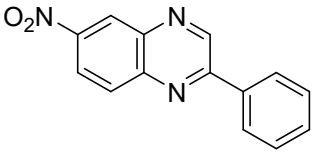

# $^{1}H$ and $^{13}C$ NMR of Compound **3i**

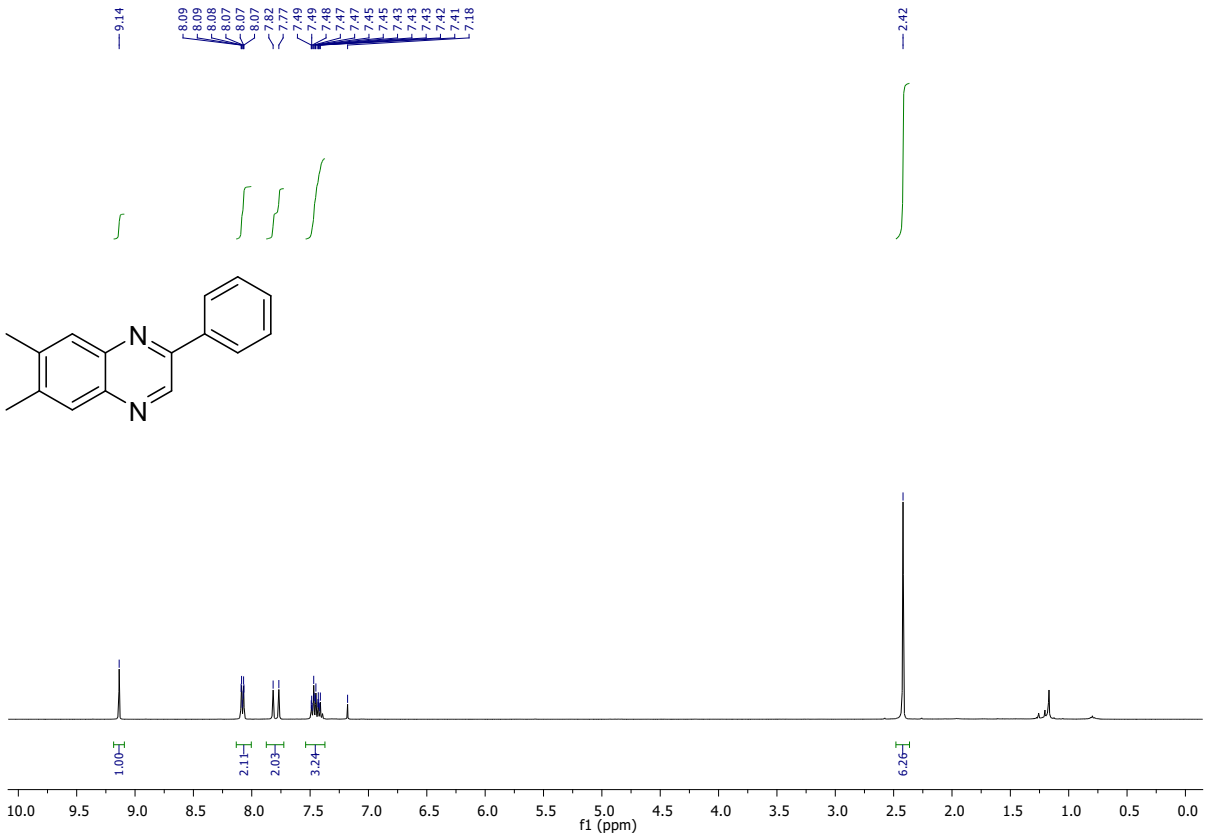


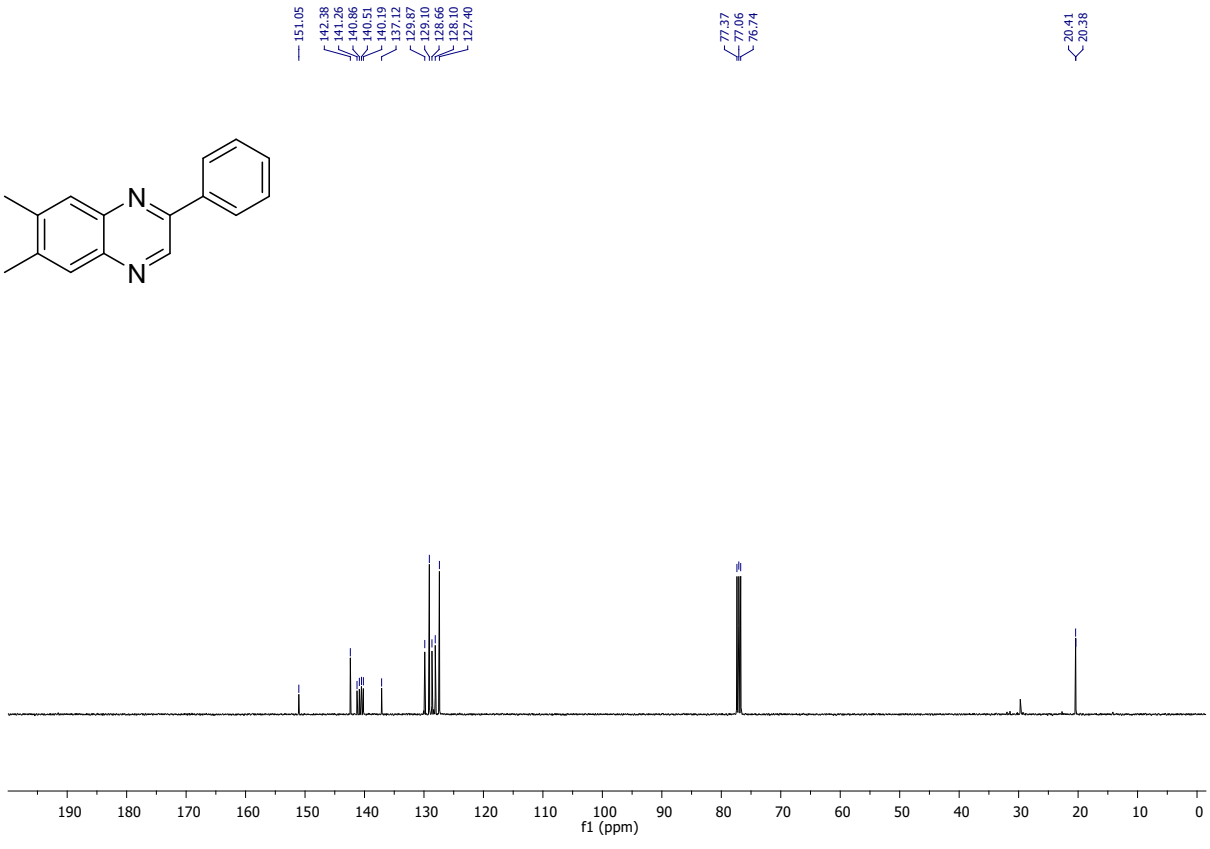

## $^{1}H$ and $^{13}C$ NMR of Compound **3j**

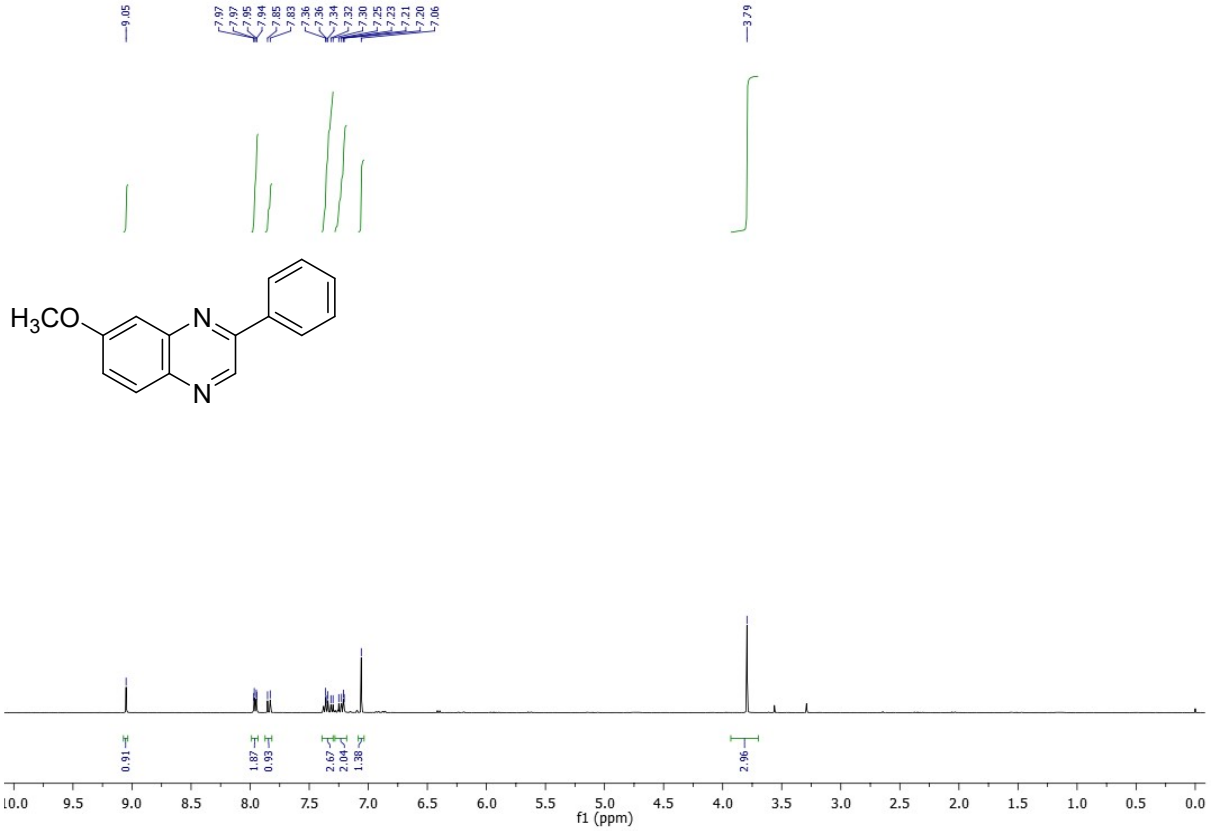


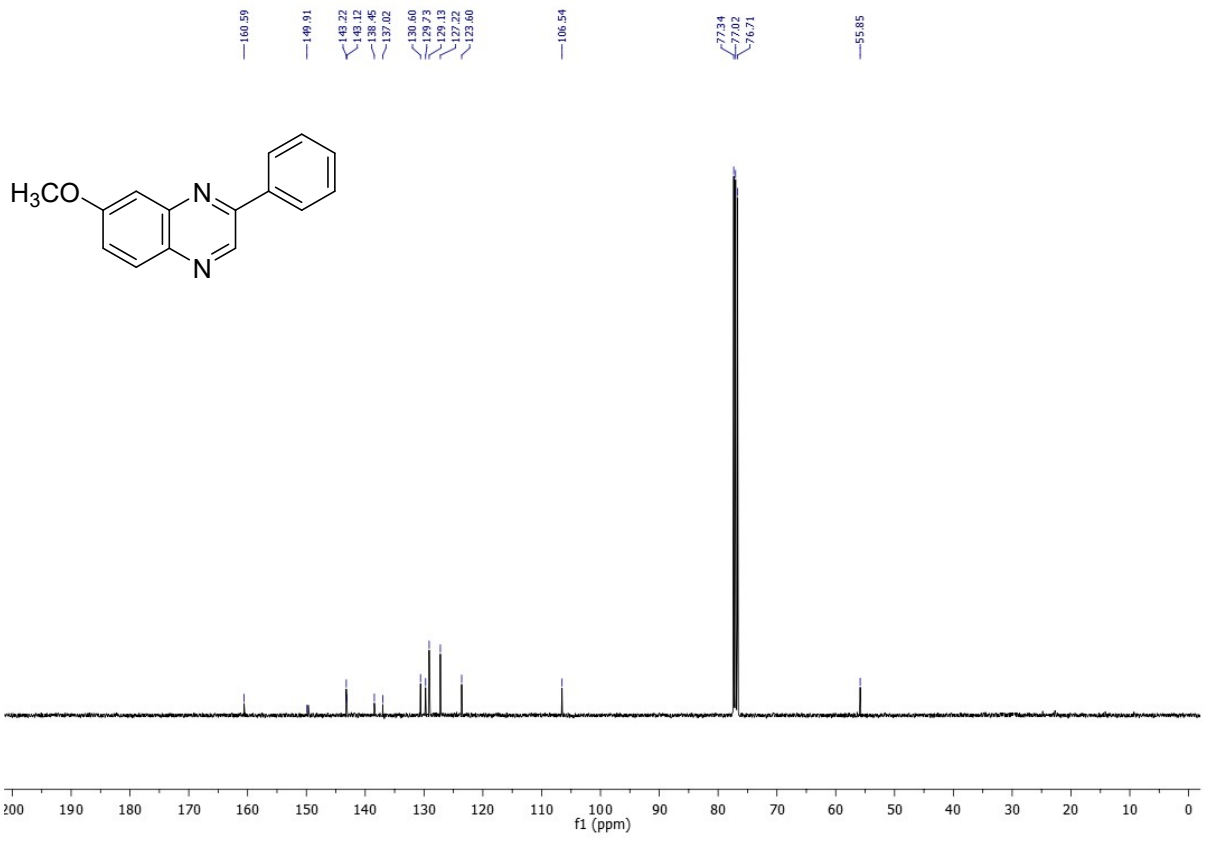

# $^{1}H$ and $^{13}C$ NMR of Compound **3k**

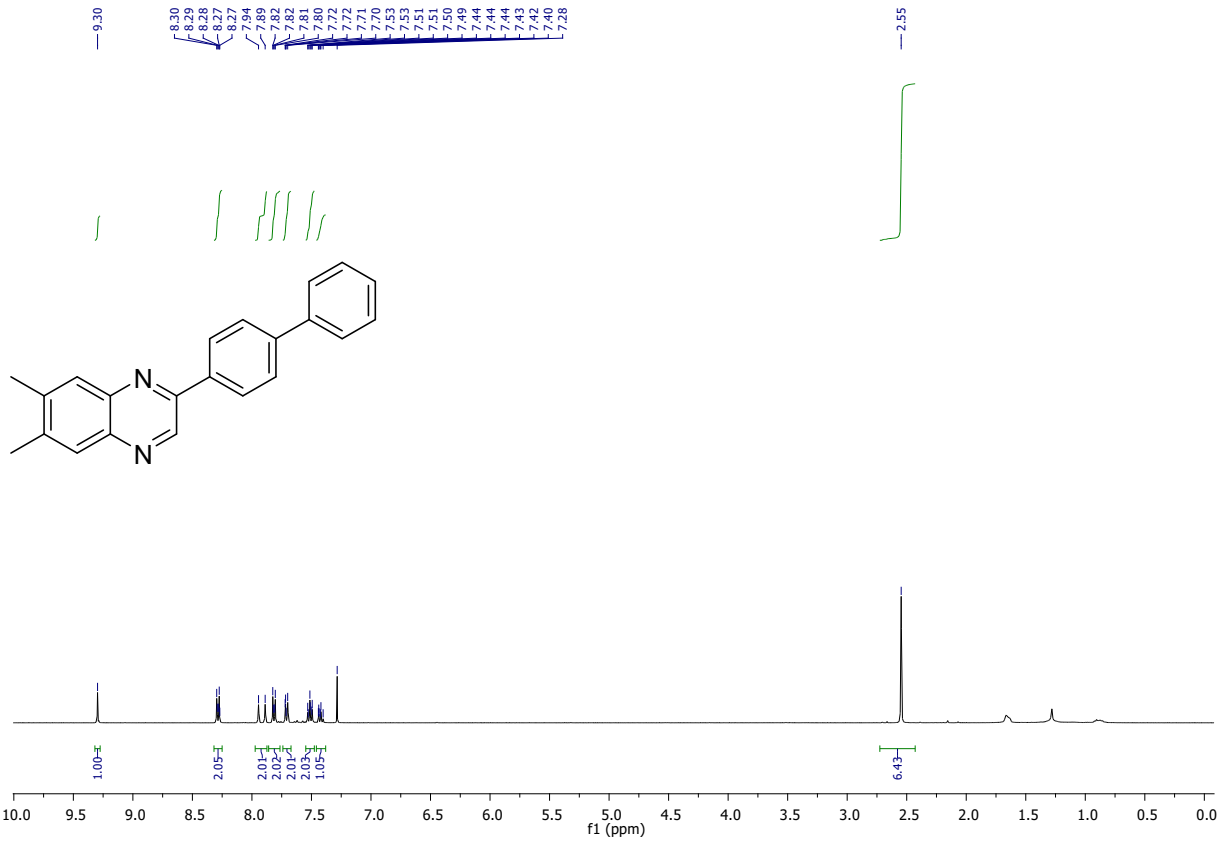


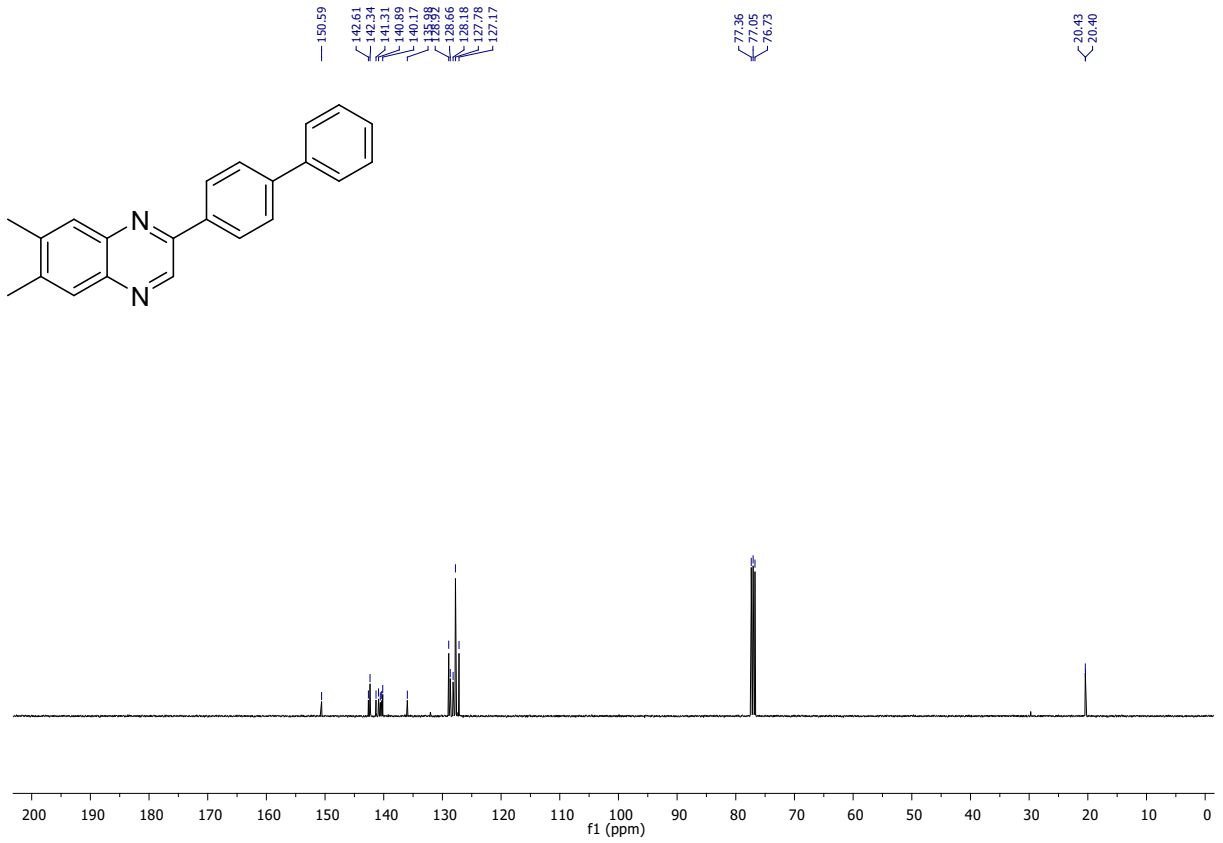

# $^{1}H$ and $^{13}C$ NMR of Compound **3l**

# $^{1}H$ and $^{13}C$ NMR of Compound **3m**

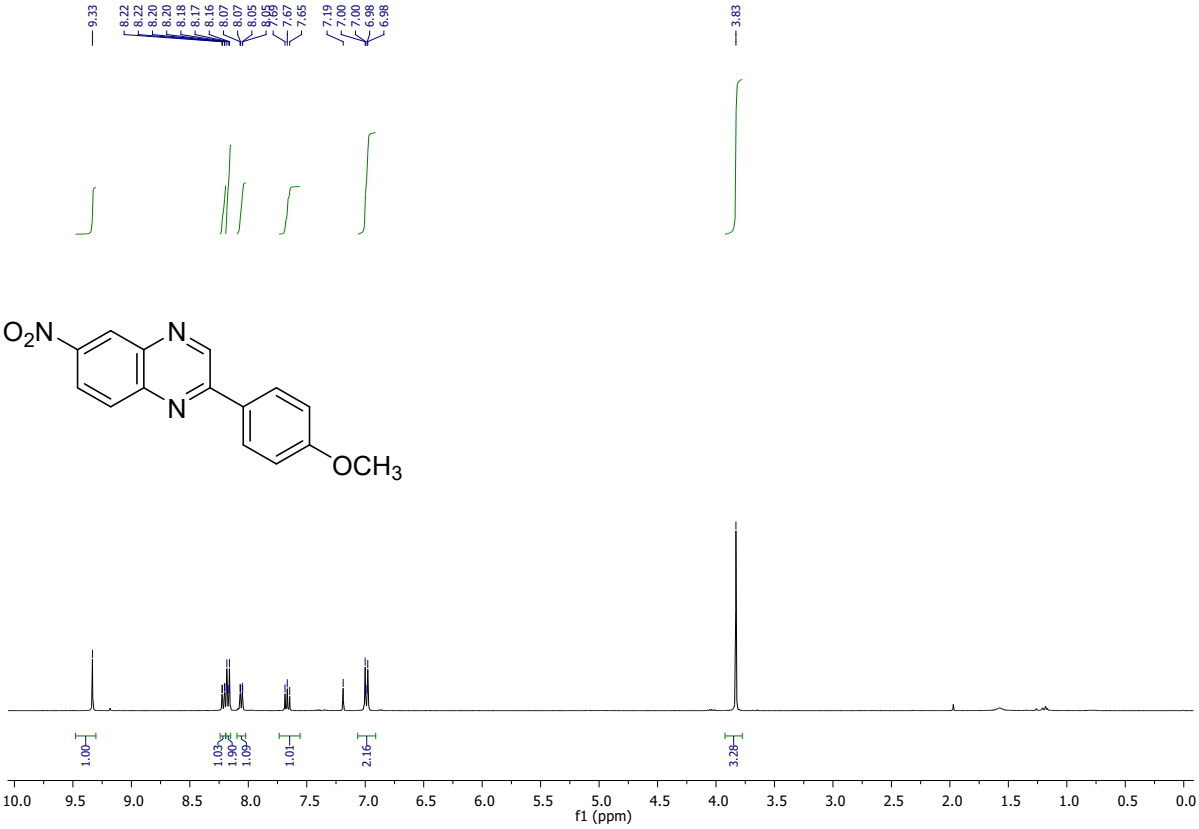


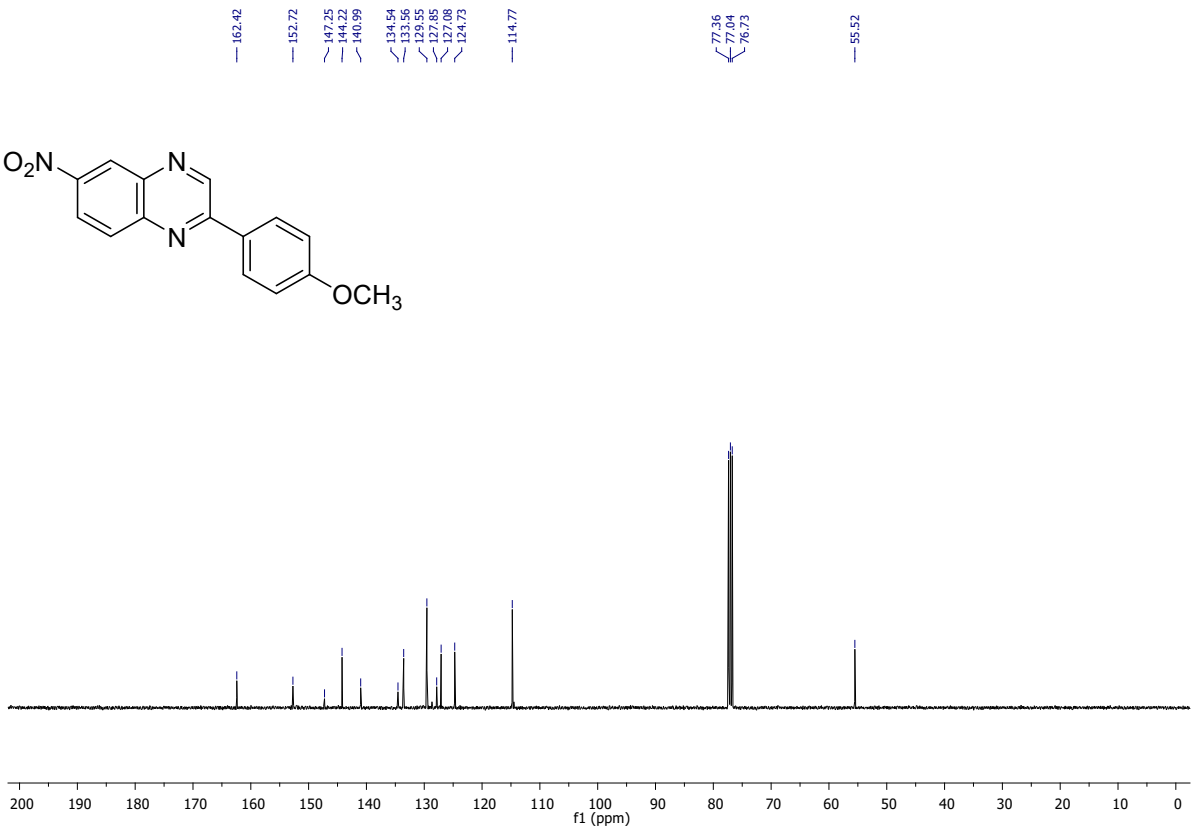

## $^{1}H$ and $^{13}C$ NMR of Compound **3n**

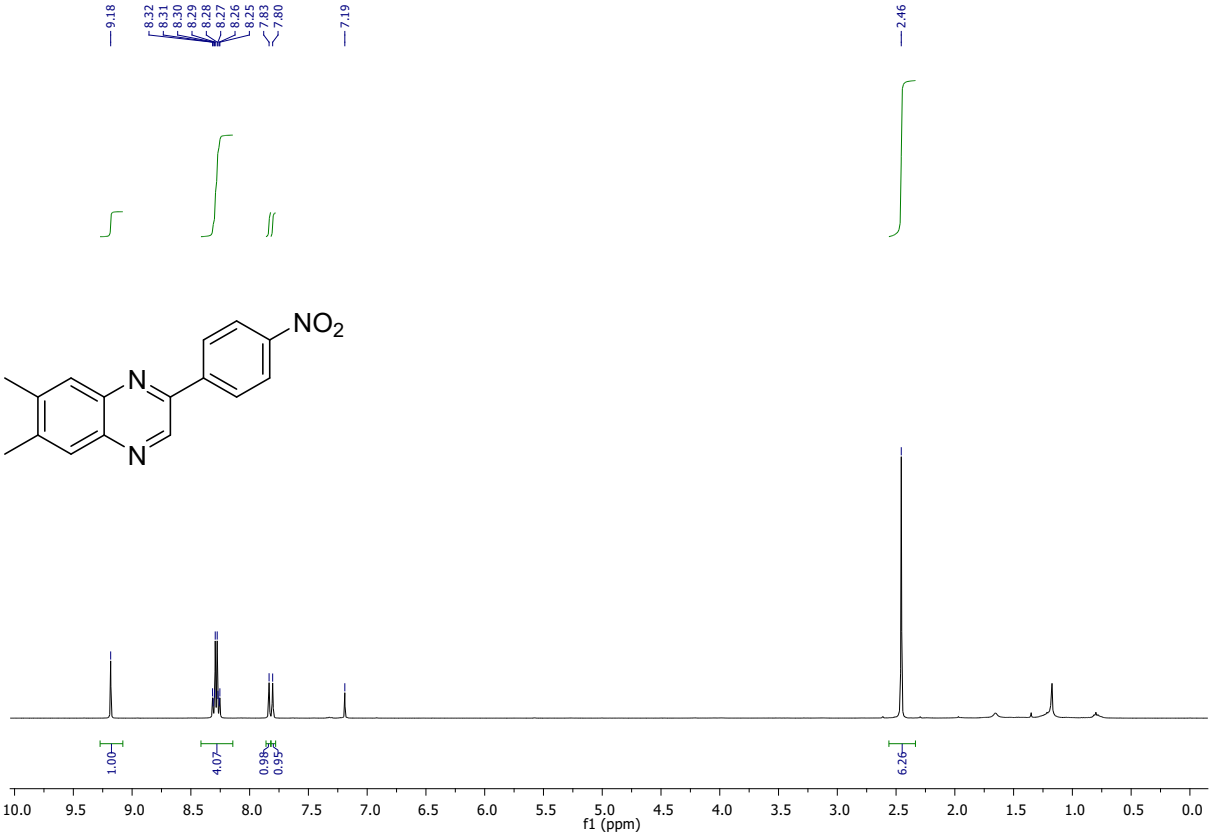


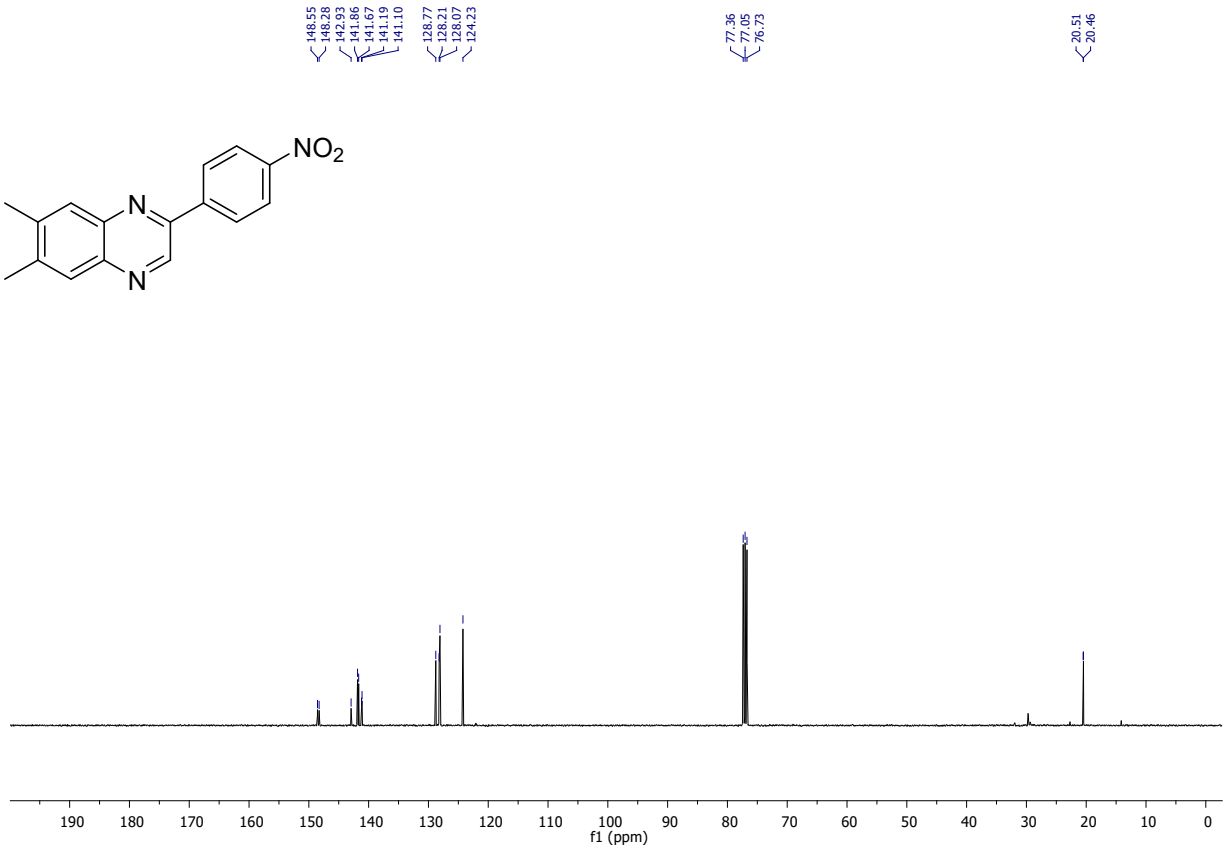

# $^{1}H$ and $^{13}C$ NMR of Compound **3o**

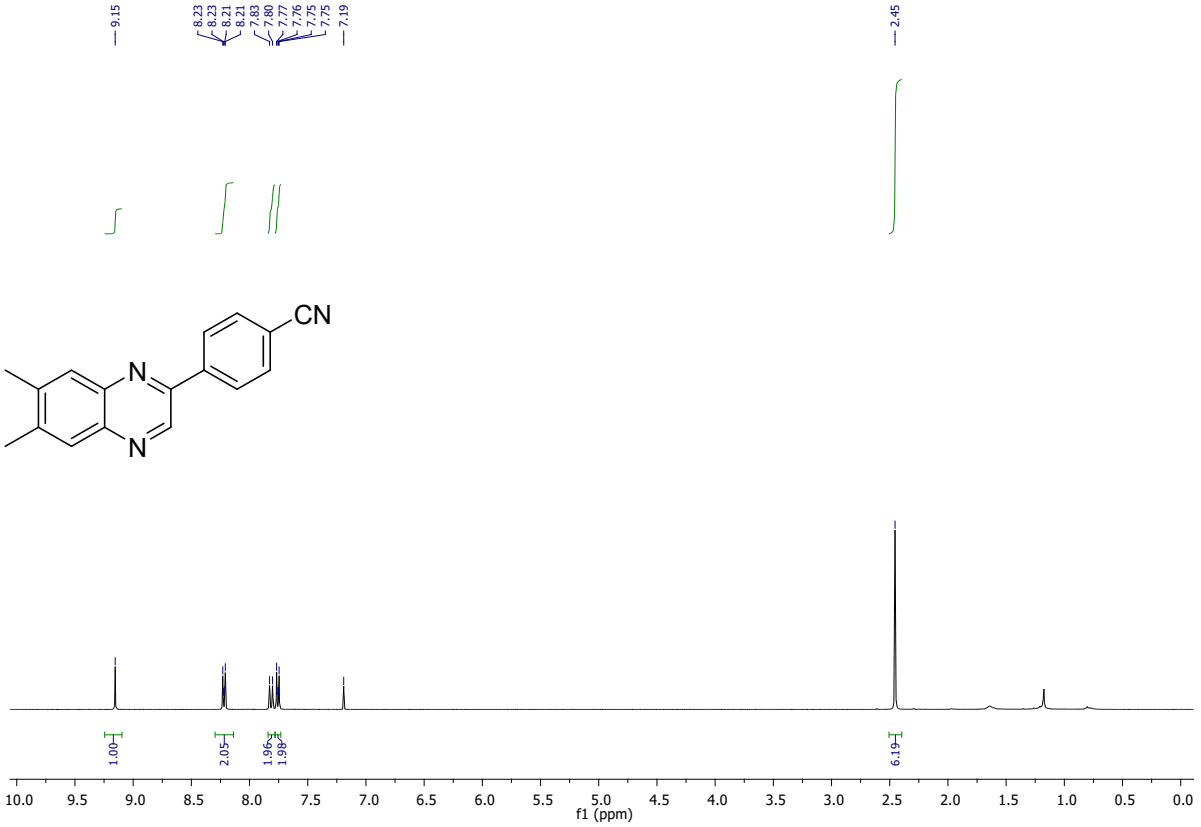


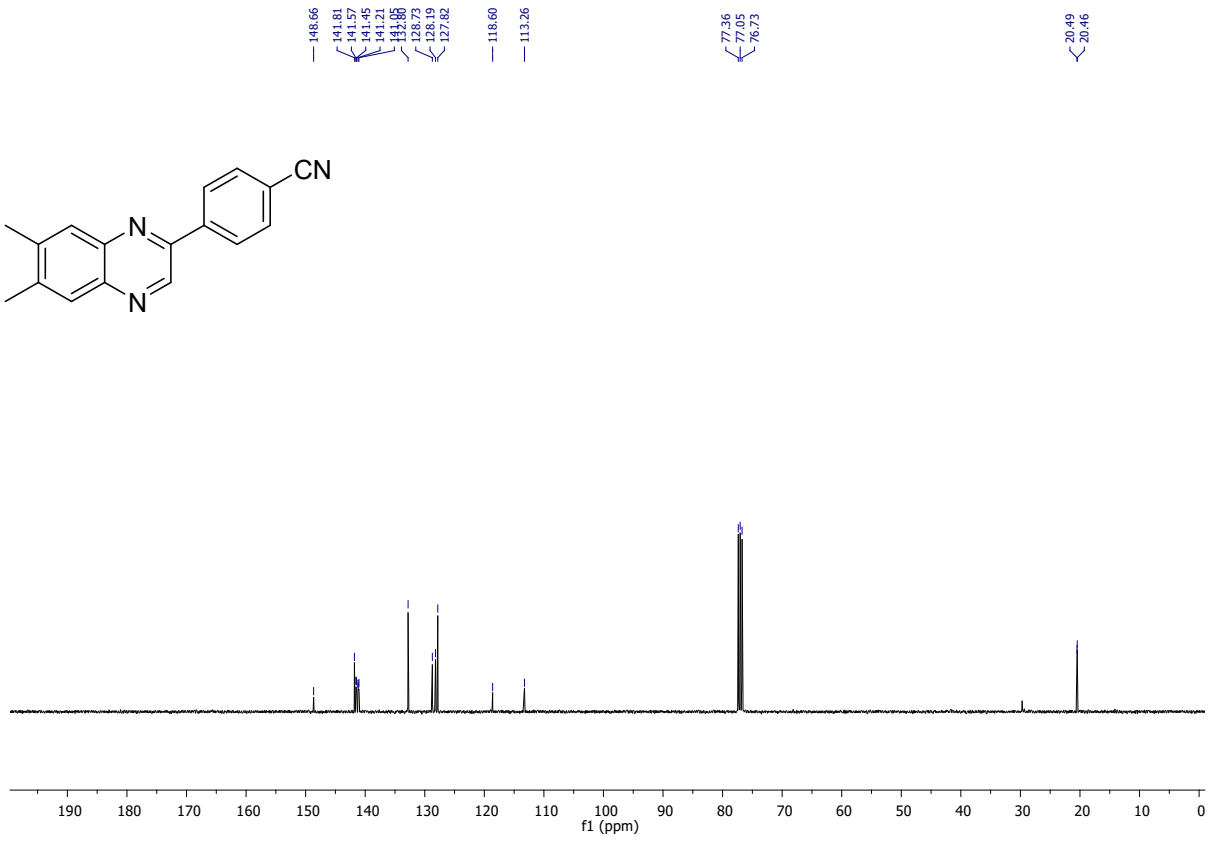

# $^{1}H$ and $^{13}C$ NMR of Compound **3p**

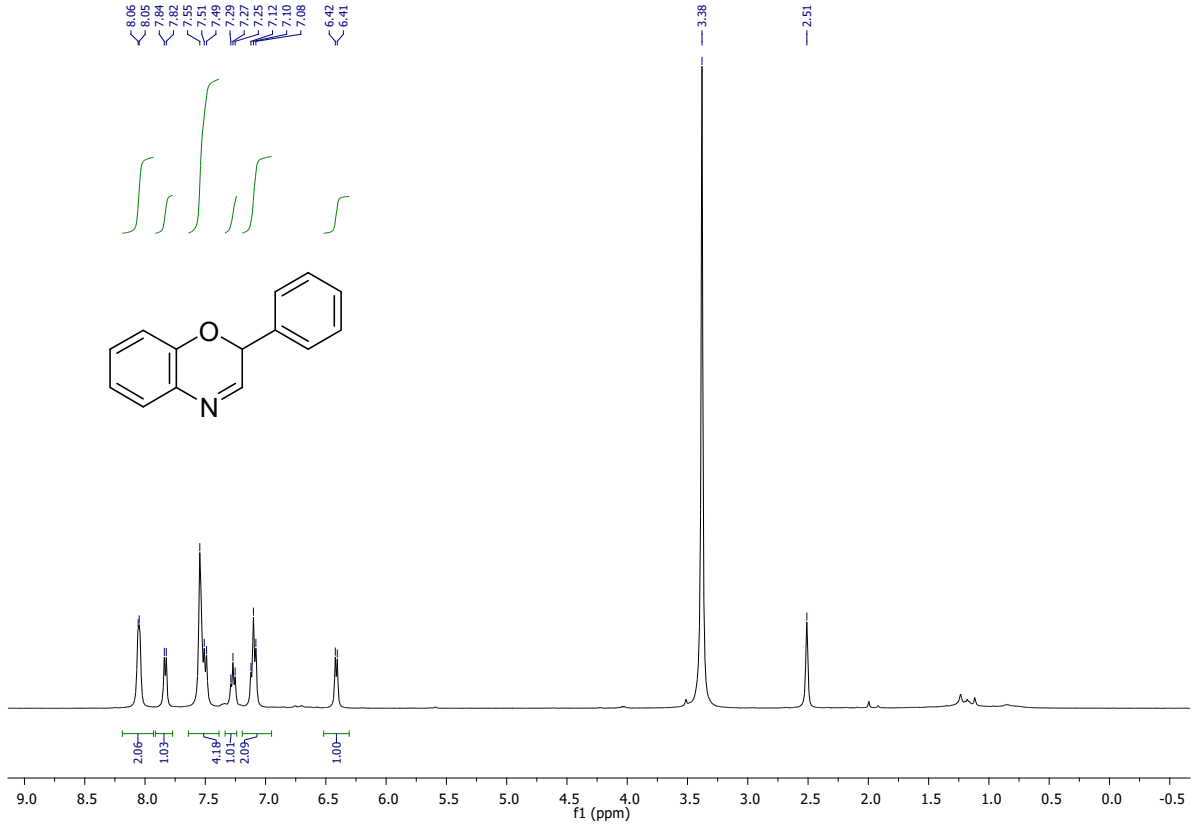


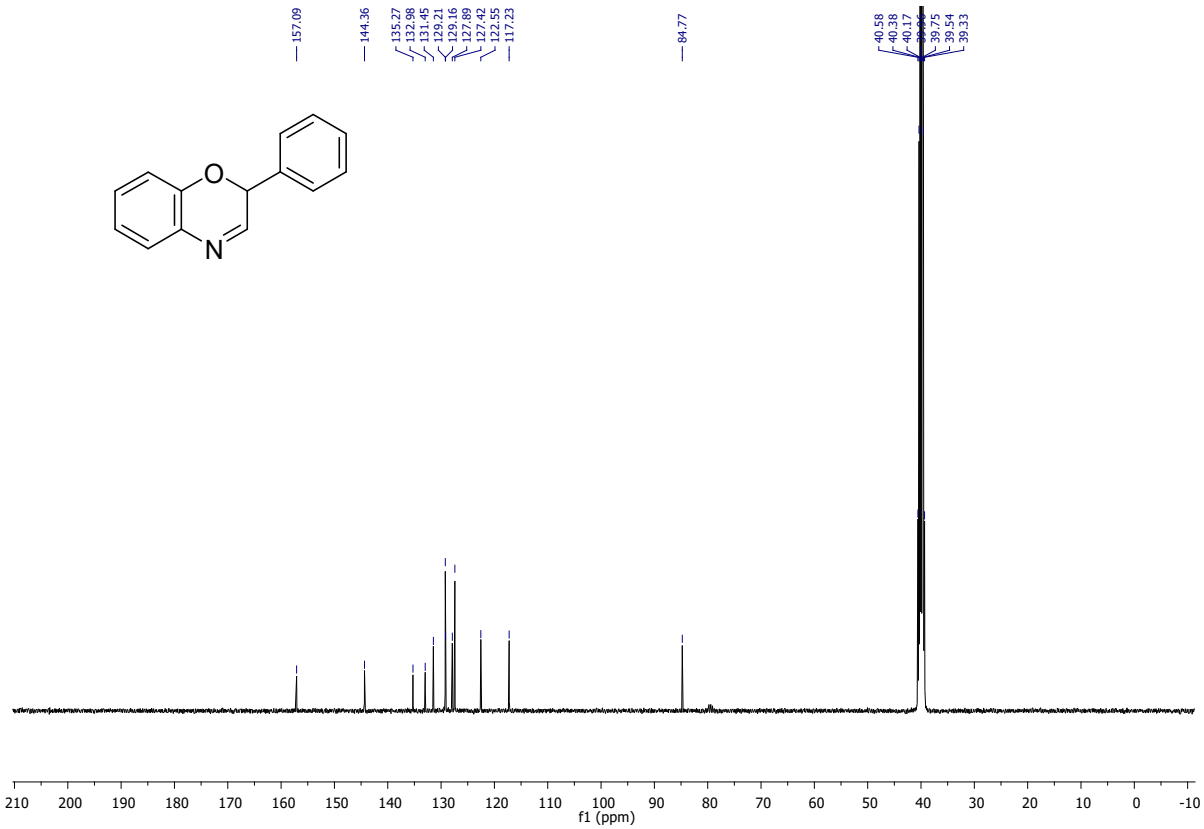

# $^{1}H$ and $^{13}C$ NMR of Compound **3q**

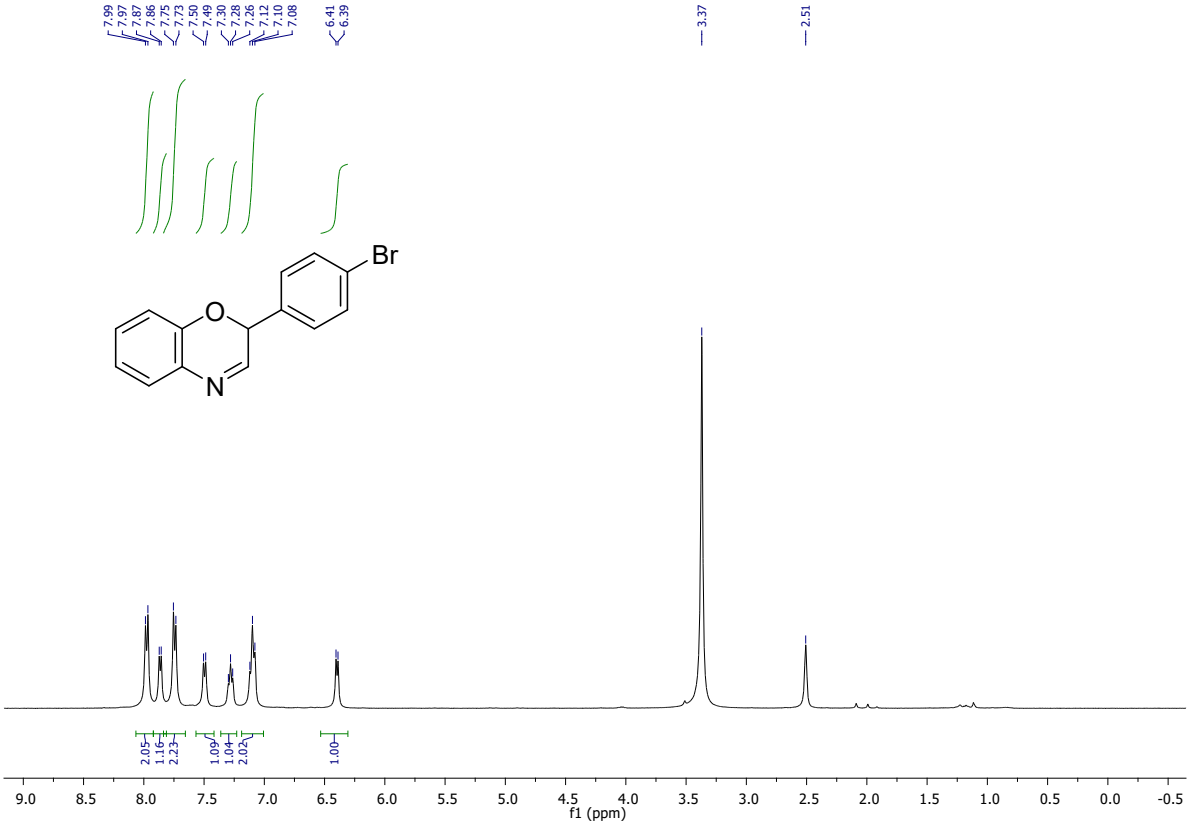


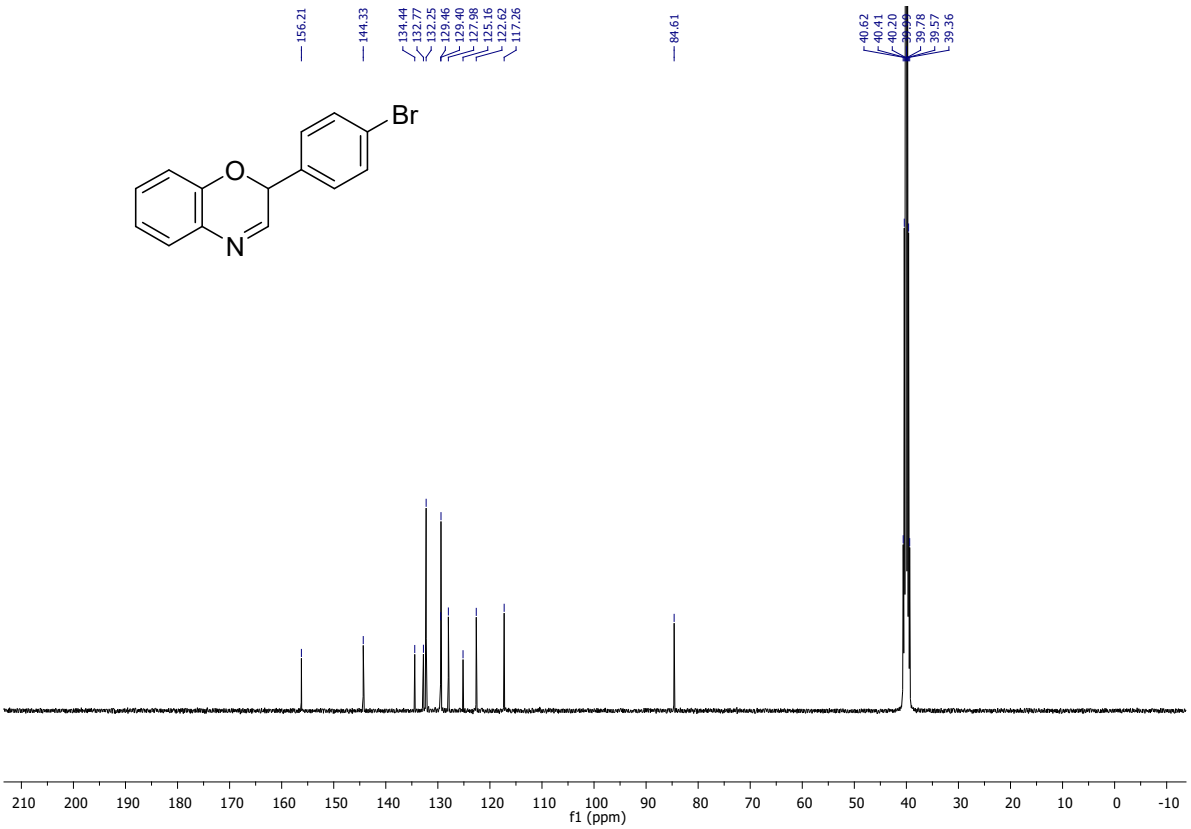

# $^{1}H$ and $^{13}C$ NMR of Compound **3r**

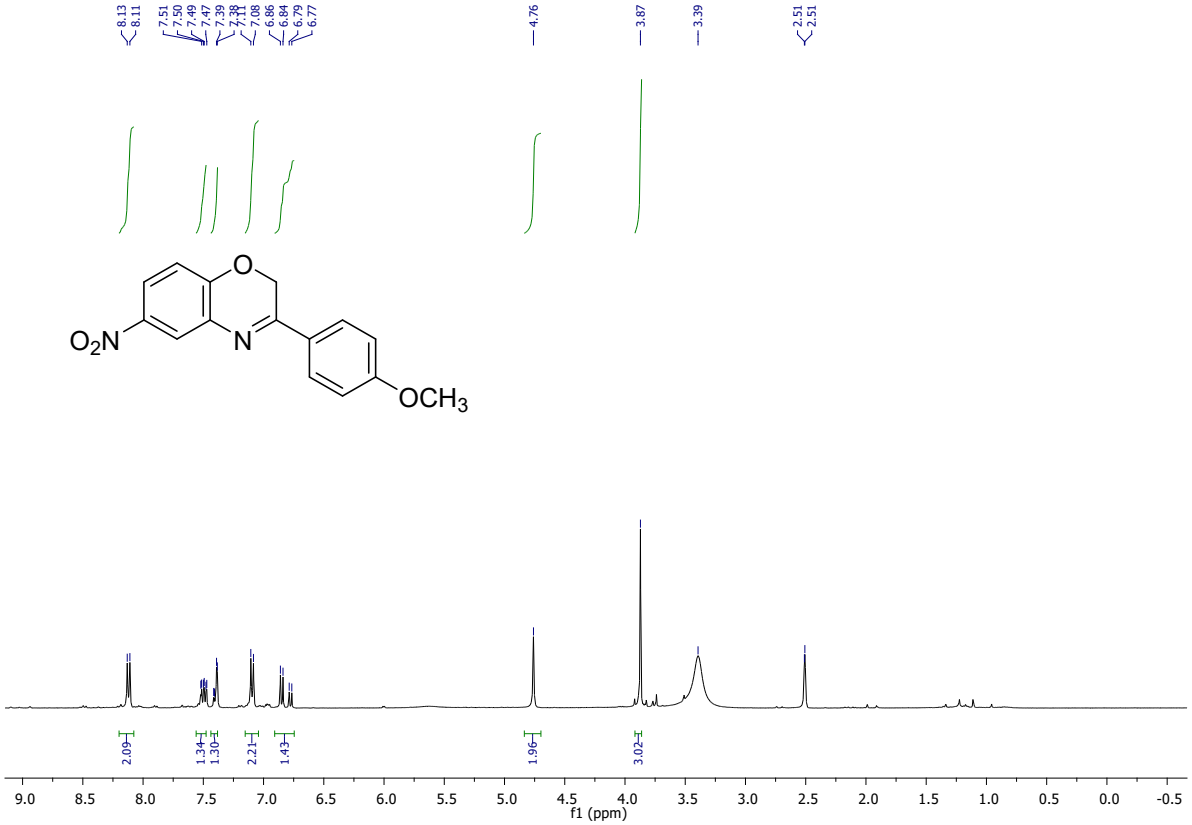


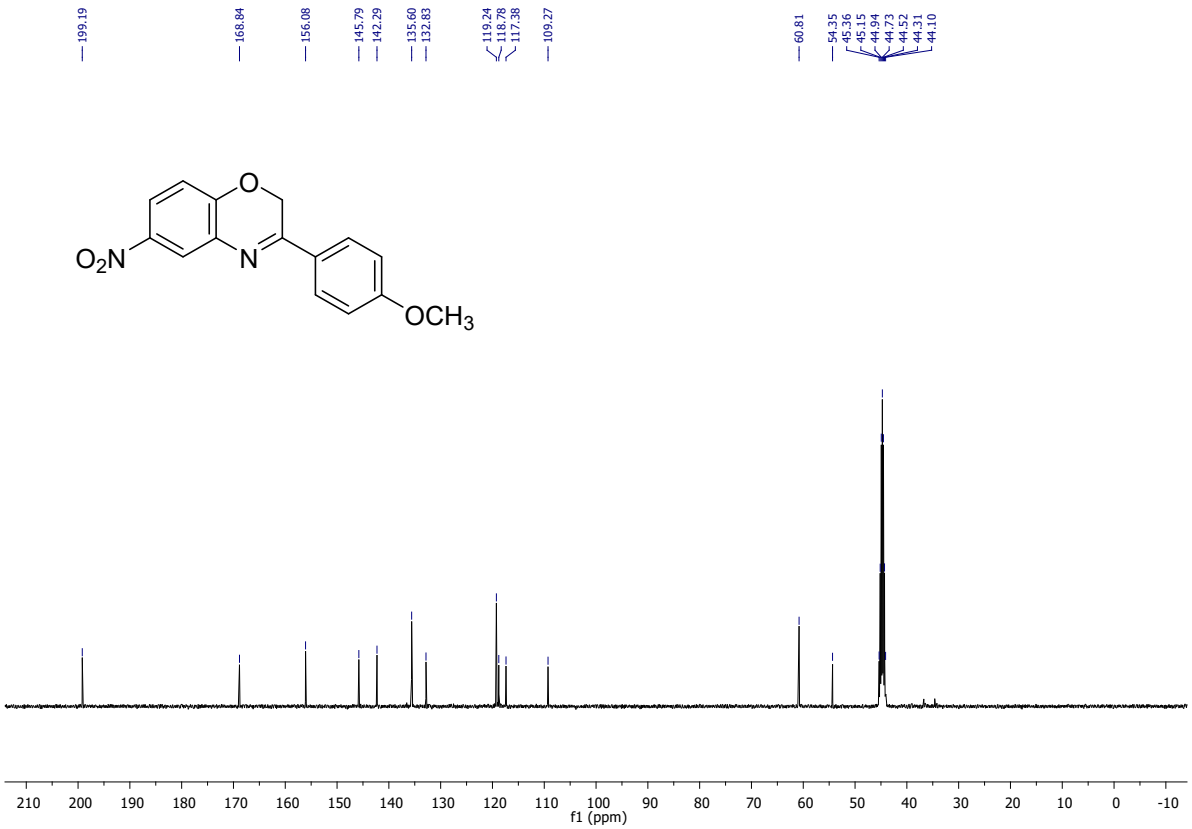

# $^{1}H$ and $^{13}C$ NMR of Compound **3s**

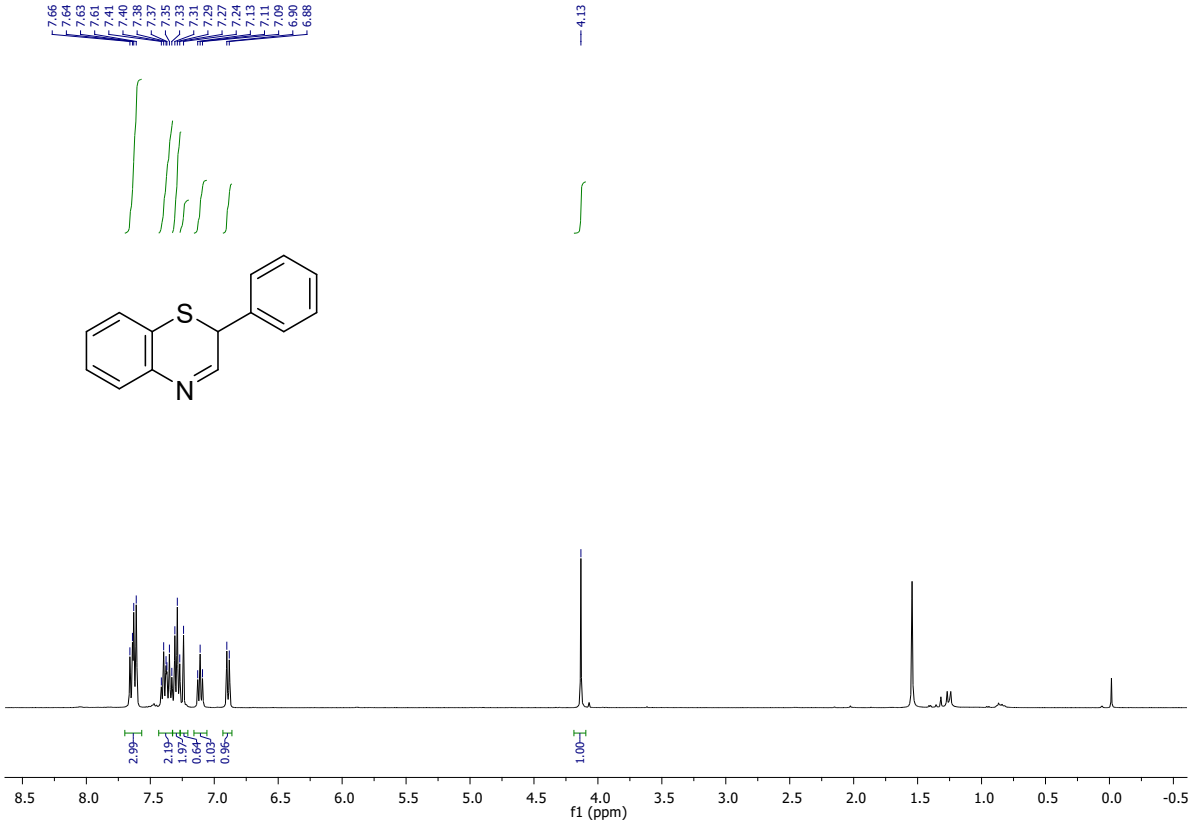


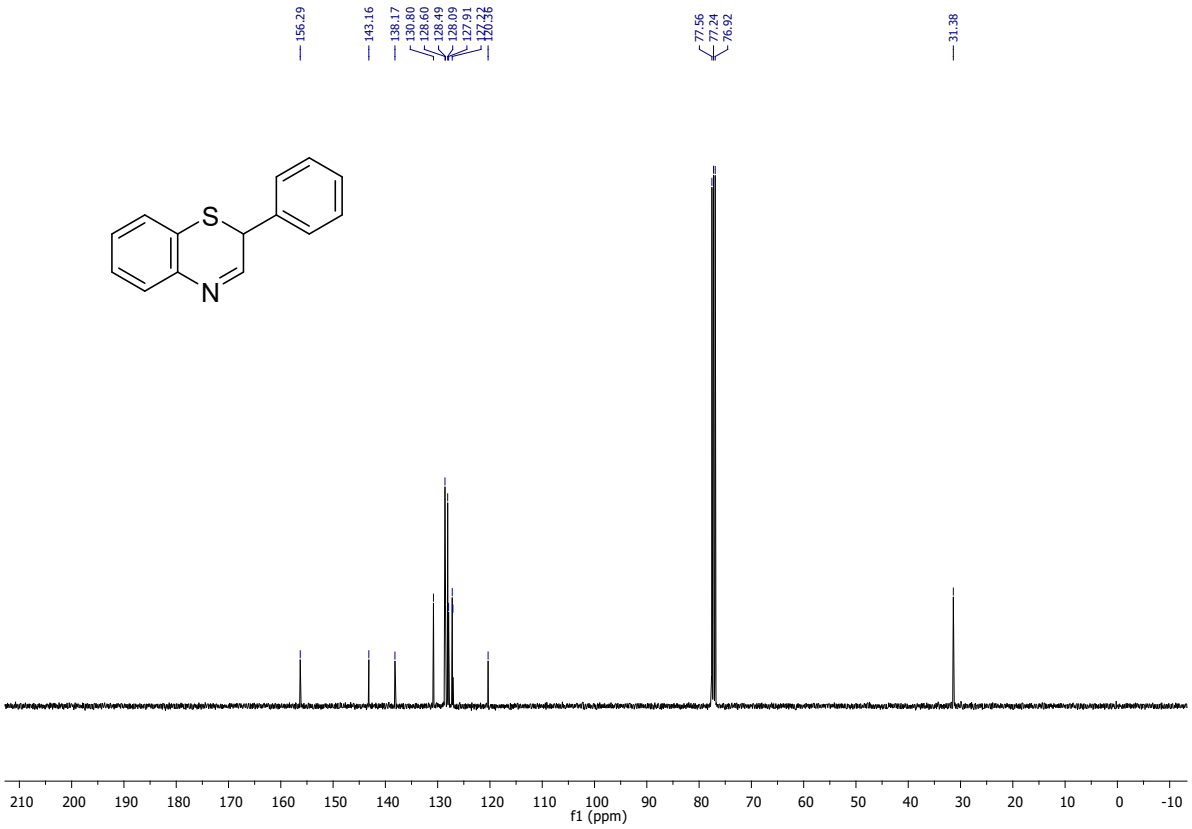

# $^{1}H$ and $^{13}C$ NMR of Compound **3t**

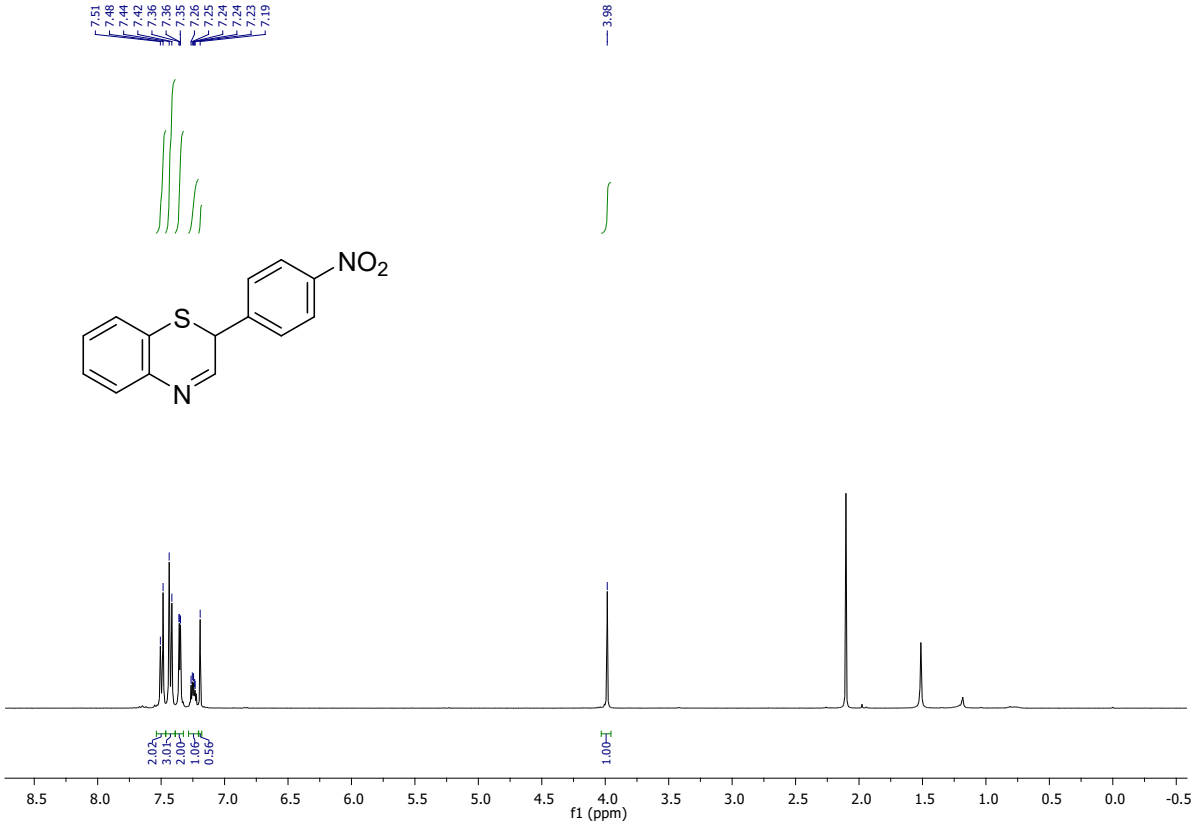


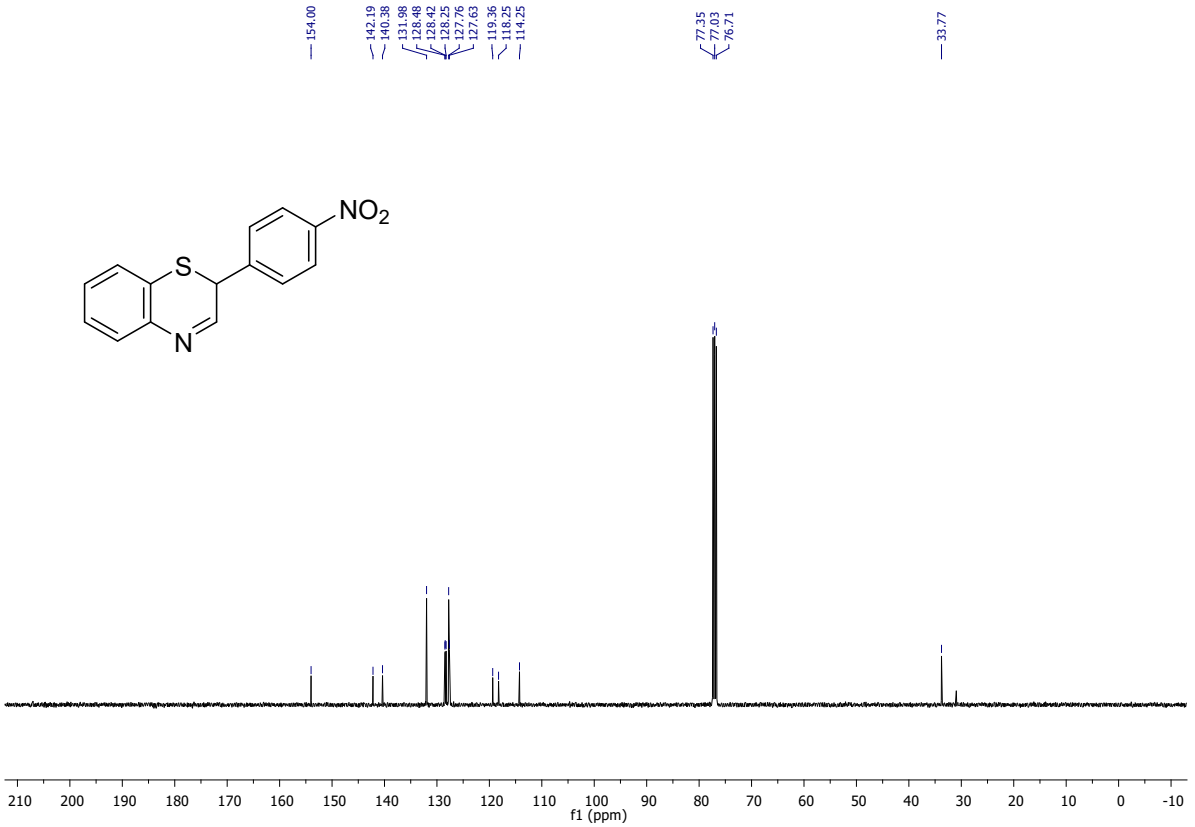

$^{1}H$ and $^{13}C$ NMR of Compound **3u**

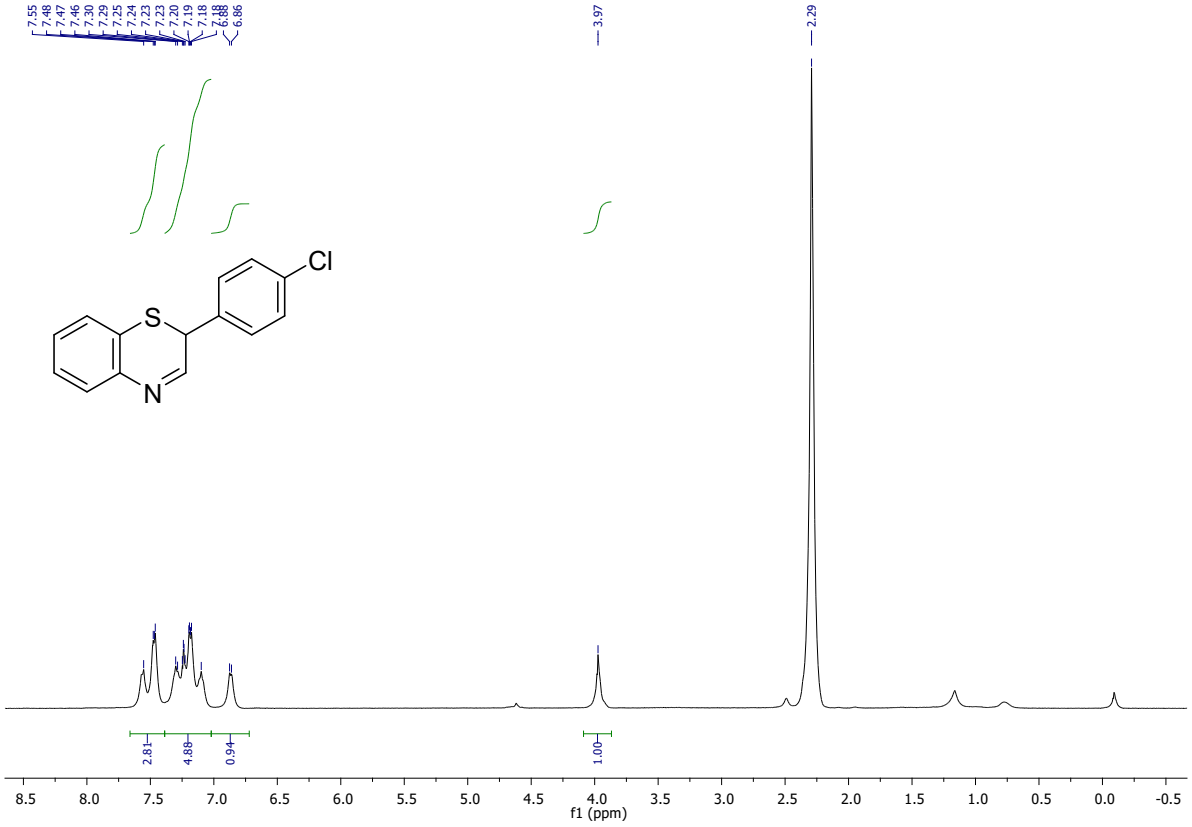


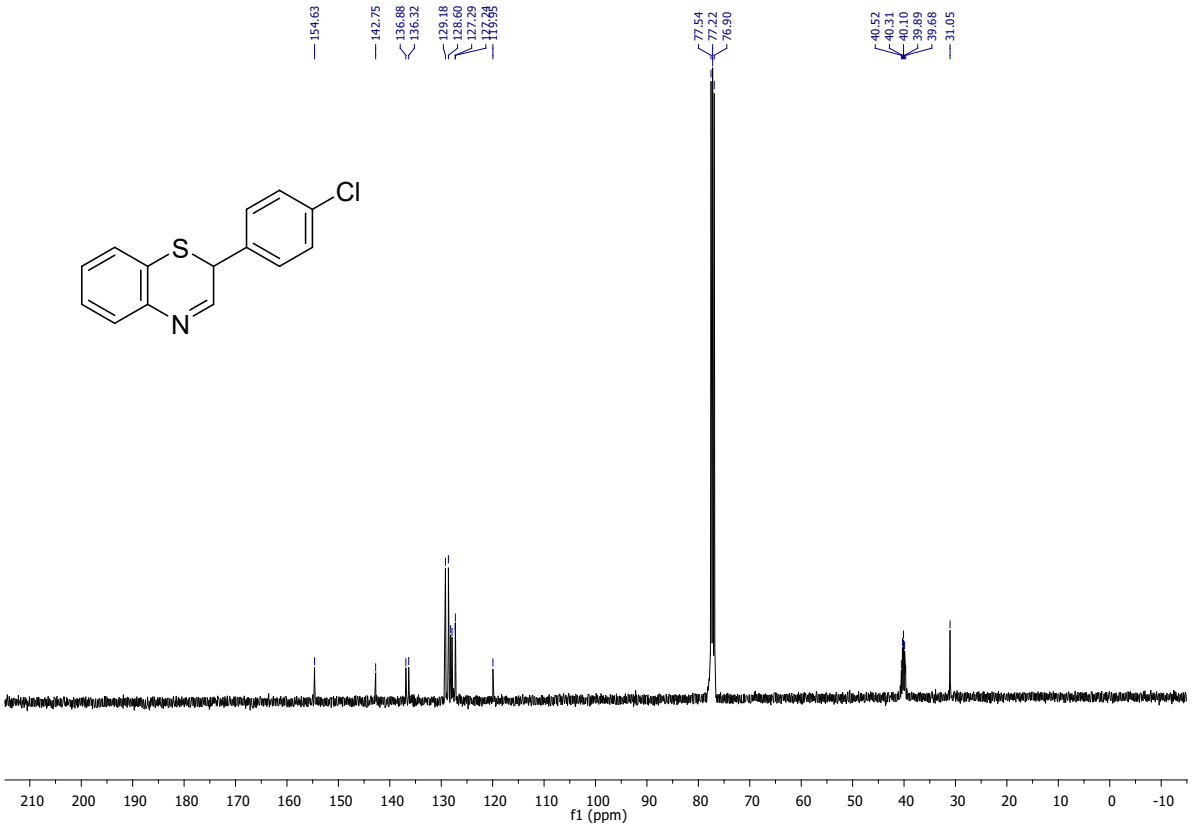

## $^{1}H$ and $^{13}C$ NMR of Compound **3v**

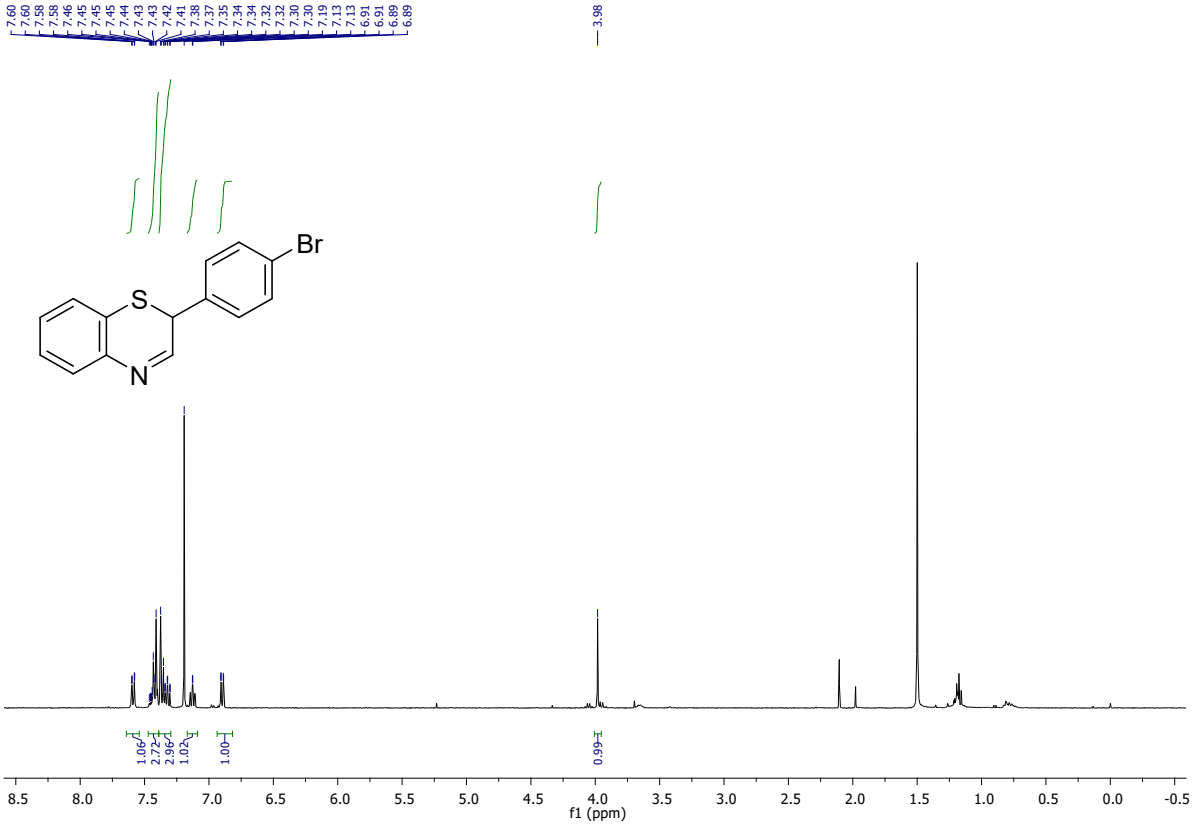


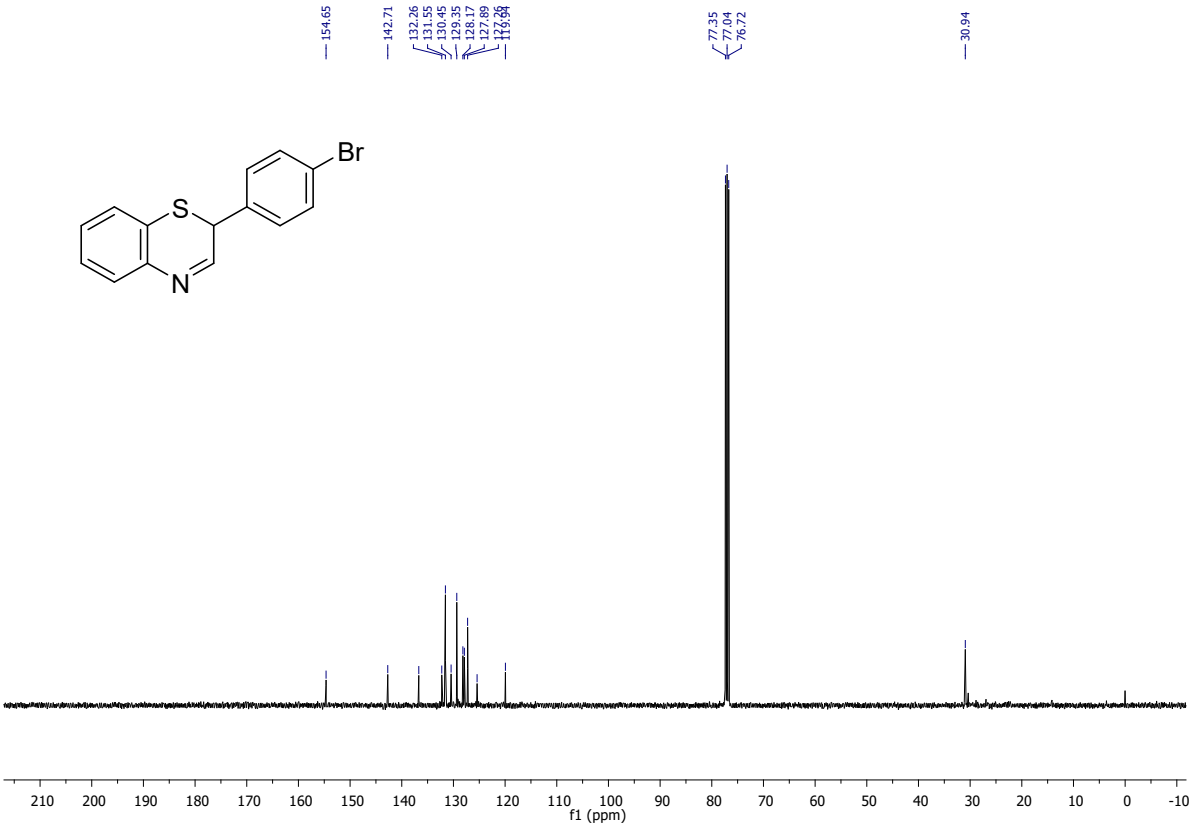

# $^{1}H$ and $^{13}C$ NMR of Compound **II**

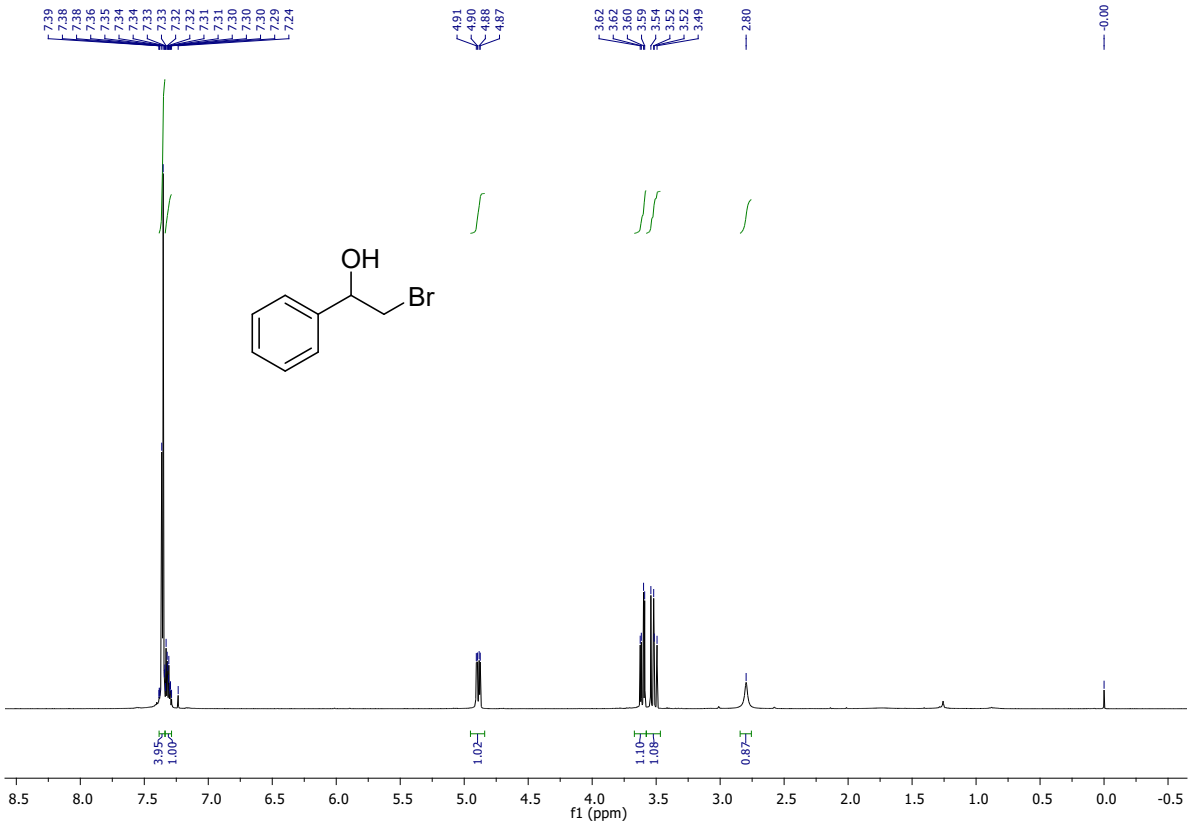


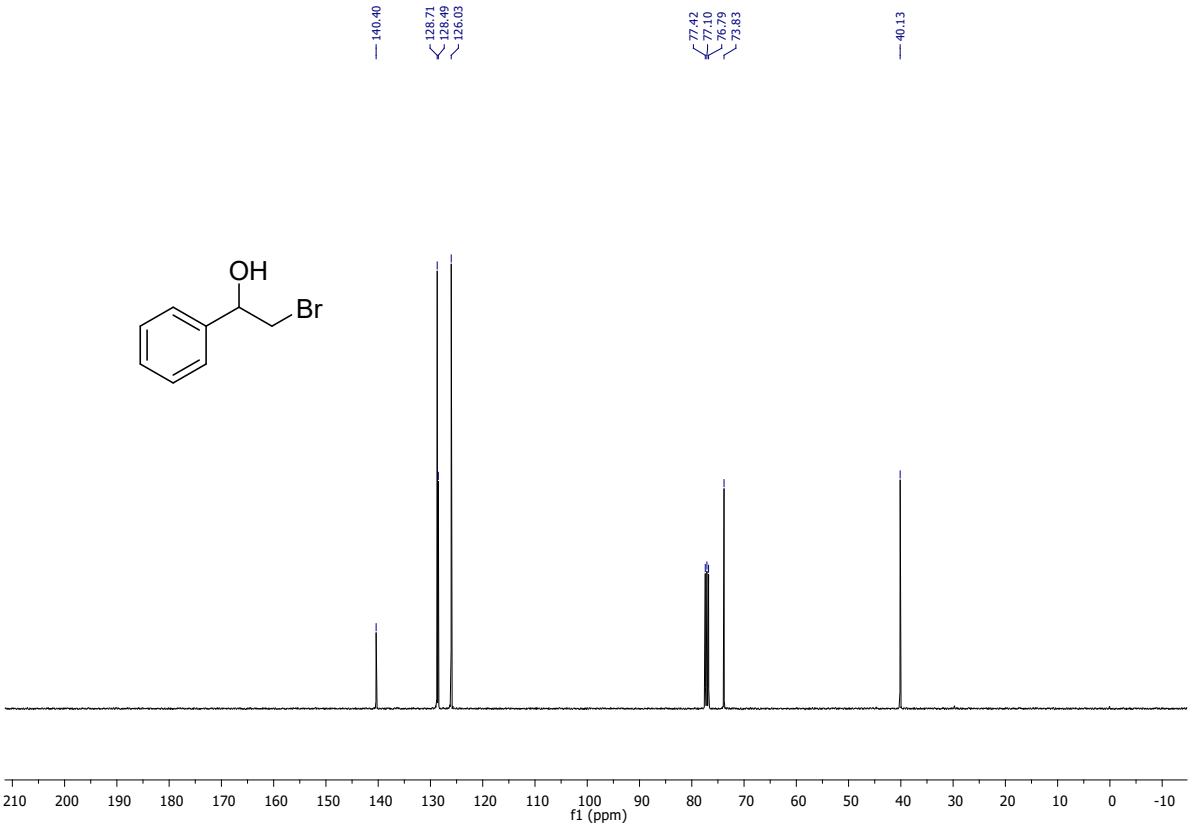

## Locus of solubilizates in micellar medium

To find the locus of the reaction site, 1.0 mM CPB solution was prepared in $D_2O$ by dissolving 7.6 mg of CPB in 20 ml of $D_2O$ on constant stirring for an hour in a clean RB flask. Various concentrations of 1,2-diaminobenzene, 0.2, 0.4, 0.8, 1.6 and 3.2 M were prepared in this micellar solution of CPB, and their proton NMR was recorded and compared with pure CPB solution in $D_2O$. With the increase in the concentration of solubilizate, 1,2-diaminobenzene, the chemical shifts of all CPB protons were tabulated and plotted in a graph to investigate its locus. Similarly, the same experiment was carried out to know the locus of another solubilizate, styrene. Proton NMR of 1.0 mM CPB micellar solution in $D_2O$ was recorded and compared with NMRs of 0.2, 0.4, 0.8, 1.6 and 3.2 M solutions of styrene in CPB solution. Change in chemical shifts was analyzed to determine its locus in micellar assembly (Table S1-S2).

**Table S1.** Chemical shift of protons in CPB in $D_2O$ at various concentrations of styrenes

| **Conc. Of styrene** | **Chemical shift of all CPB protons at various conc. Of styrene** | | | | | | | |
|---|---|---|---|---|---|---|---|---|
| | **(a, a')-CH** | **(b, b') -CH** | **c-CH** | **α-$CH_2$** | **β-$CH_2$** | **γ-$CH_2$** | **Δ-$(CH_2)_{12}$** | **-$CH_3$** |
| 0.00M | 9.02 | 8.10 | 8.56 | 4.68 | 1.98 | 1.29 | 1.08 | 0.68 |
| 0.02M | 8.97 | 8.08 | 8.56 | 4.67 | 1.94 | 1.25 | 1.10 | 0.70 |
| 0.04M | 8.94 | 8.07 | 8.55 | 4.63 | 1.90 | 1.23 | 1.10 | 0.70 |
| 0.08M | 8.93 | 8.06 | 8.53 | 4.63 | 1.90 | 1.22 | 1.10 | 0.70 |
| 0.16M | 8.89 | 8.05 | 8.53 | 4.63 | 1.87 | 1.20 | 1.10 | 0.70 |
| 0.32M | 8.89 | 8.04 | 8.52 | 4.60 | 1.86 | 1.19 | 1.09 | 0.71 |

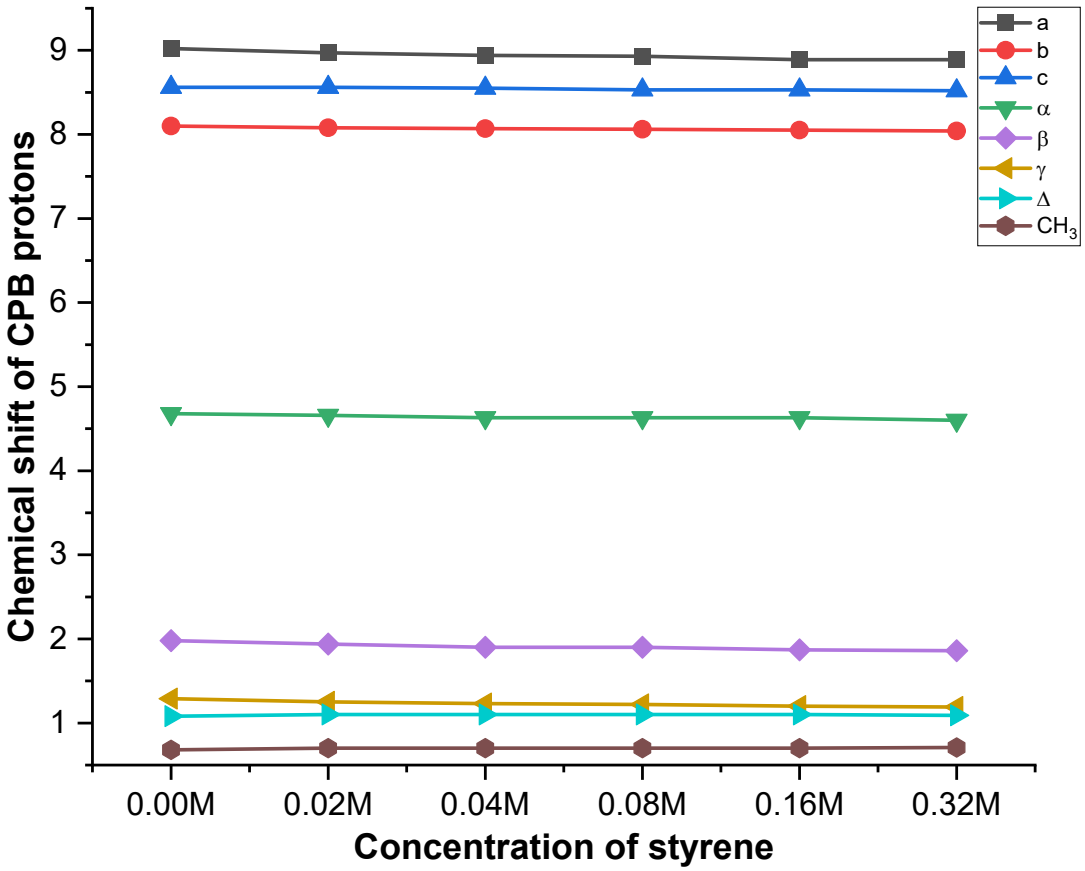


**Figure S1.** Chemical shift of protons in CPB in $D_2O$ at various concentrations of styrenes

**Table S2**. Extent of change in chemical shift ($\delta_0$ - $\delta x$) of all CPB protons at various concentrations of styrenes

| $\delta_0 - \delta_x$ | (a, a') -CH | (b, b') -CH | c-CH | α-$CH_2$ | β-$CH_2$ | γ-$CH_2$ | Δ-$(CH_2)_{12}$ | -$CH_3$ |
|---|---|---|---|---|---|---|---|---|
| $\delta_0$ - $\delta_{0.02}$ | 0.05 | 0.02 | 0.00 | 0.01 | 0.04 | 0.04 | -0.02 | -0.02 |
| $\delta_0$ - $\delta_{0.04}$ | 0.08 | 0.03 | 0.01 | 0.05 | 0.08 | 0.06 | -0.02 | -0.02 |
| $\delta_0$ - $\delta_{0.08}$ | 0.09 | 0.04 | 0.03 | 0.05 | 0.08 | 0.07 | -0.02 | -0.02 |
| $\delta_0$ - $\delta_{0.16}$ | 0.13 | 0.05 | 0.03 | 0.05 | 0.11 | 0.09 | -0.02 | -0.02 |
| $\delta_0$ - $\delta_{0.32}$ | 0.13 | 0.06 | 0.04 | 0.08 | 0.12 | 0.10 | -0.02 | -0.02 |

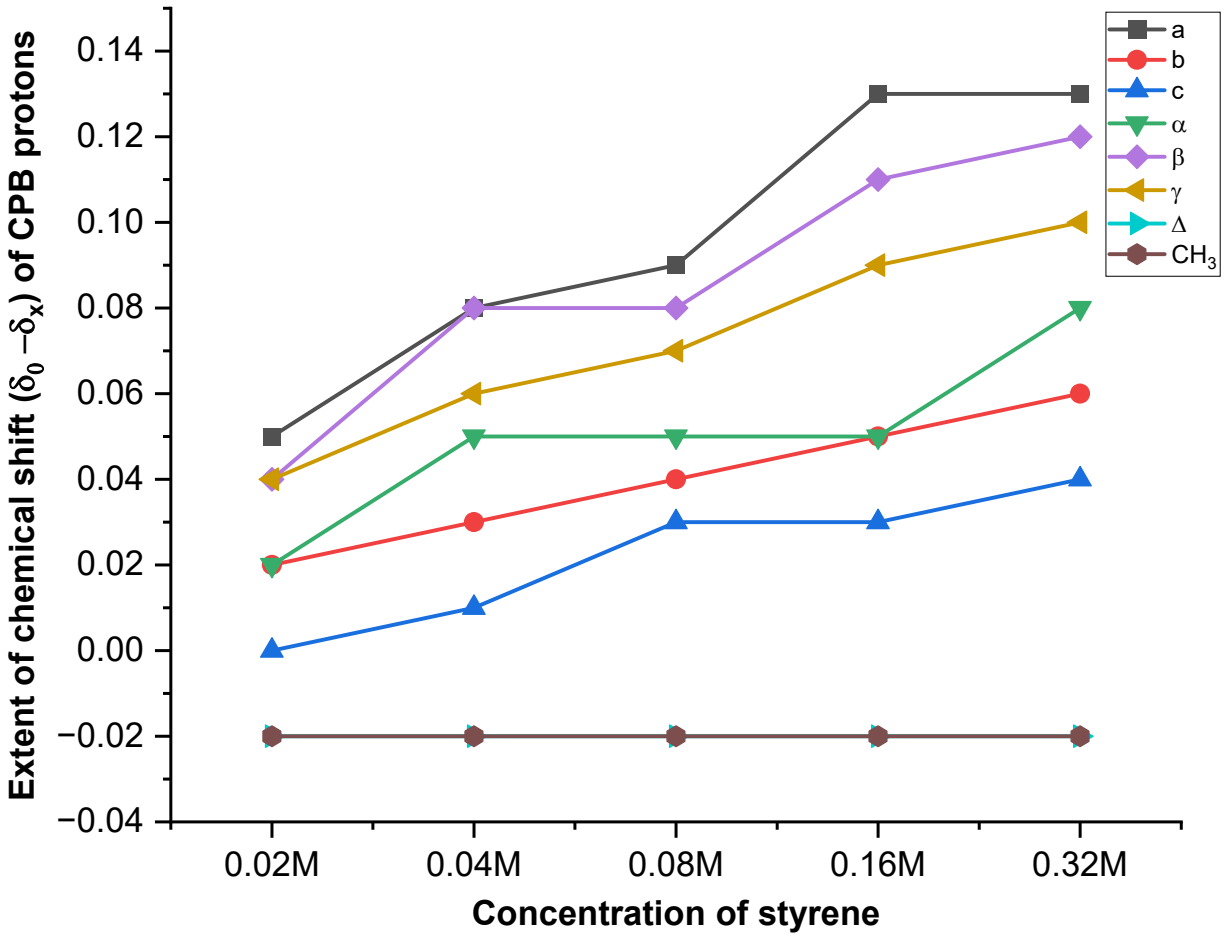


**Figure S2**. Extent of change in chemical shift ($\delta_0$ - δx) of all CPB protons at various concentrations of styrenes

## NMR study to determine locus of the reaction in CPB

**$^1$H NMR of CPB and various concentrations of solubilizates**

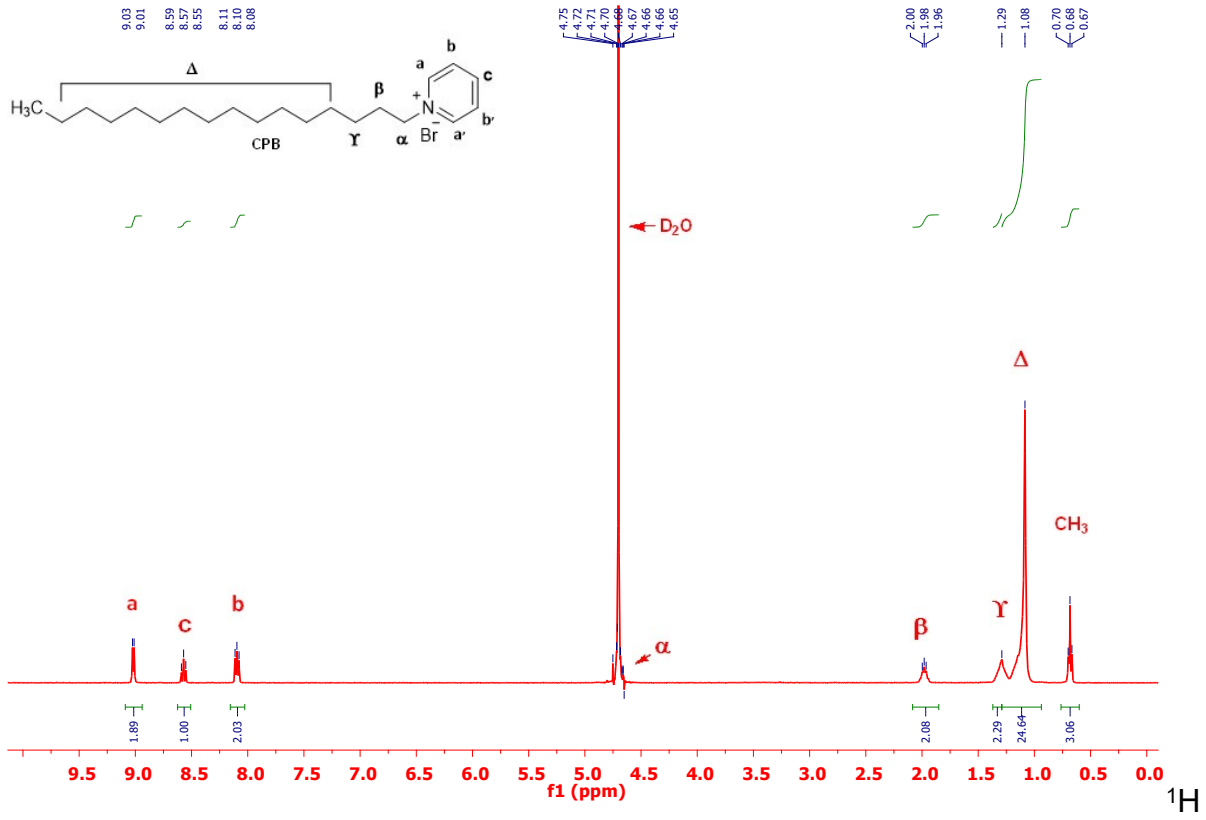

**$^1$H** NMR of CPB & 0.02M 1,2-diaminobenzene

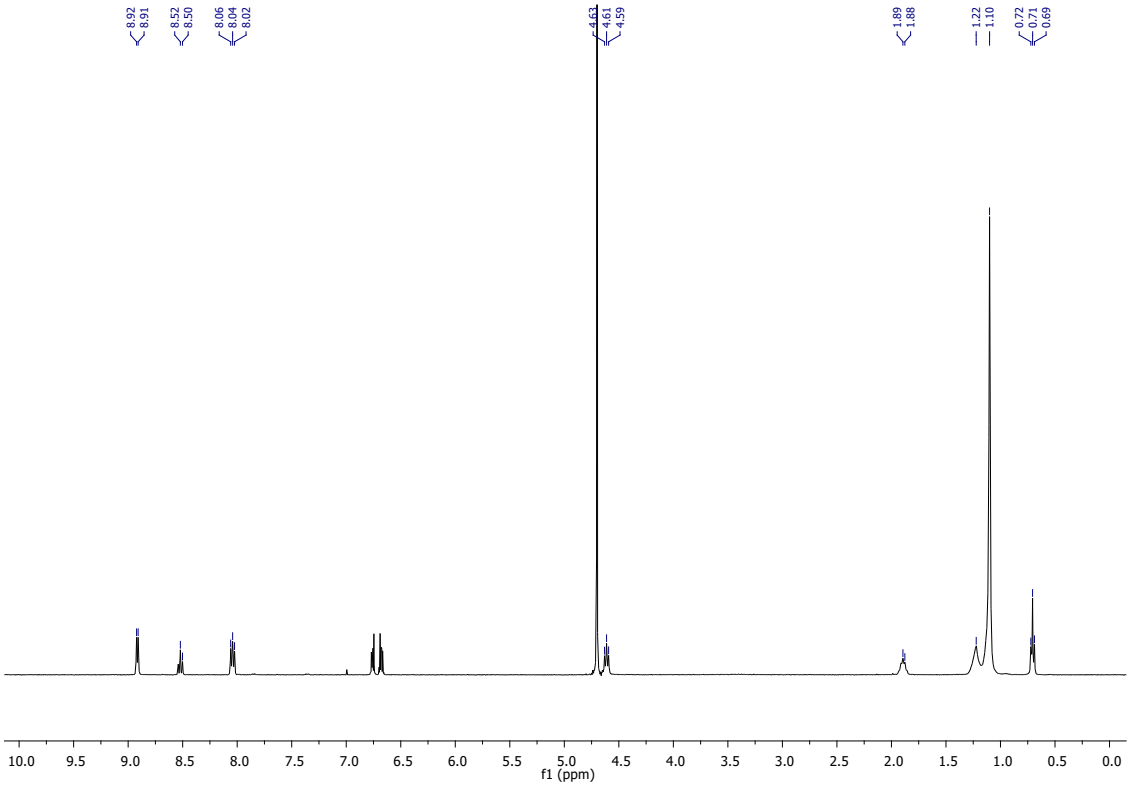


$^1$H NMR of CPB & 0.04M 1,2-diaminobenzene

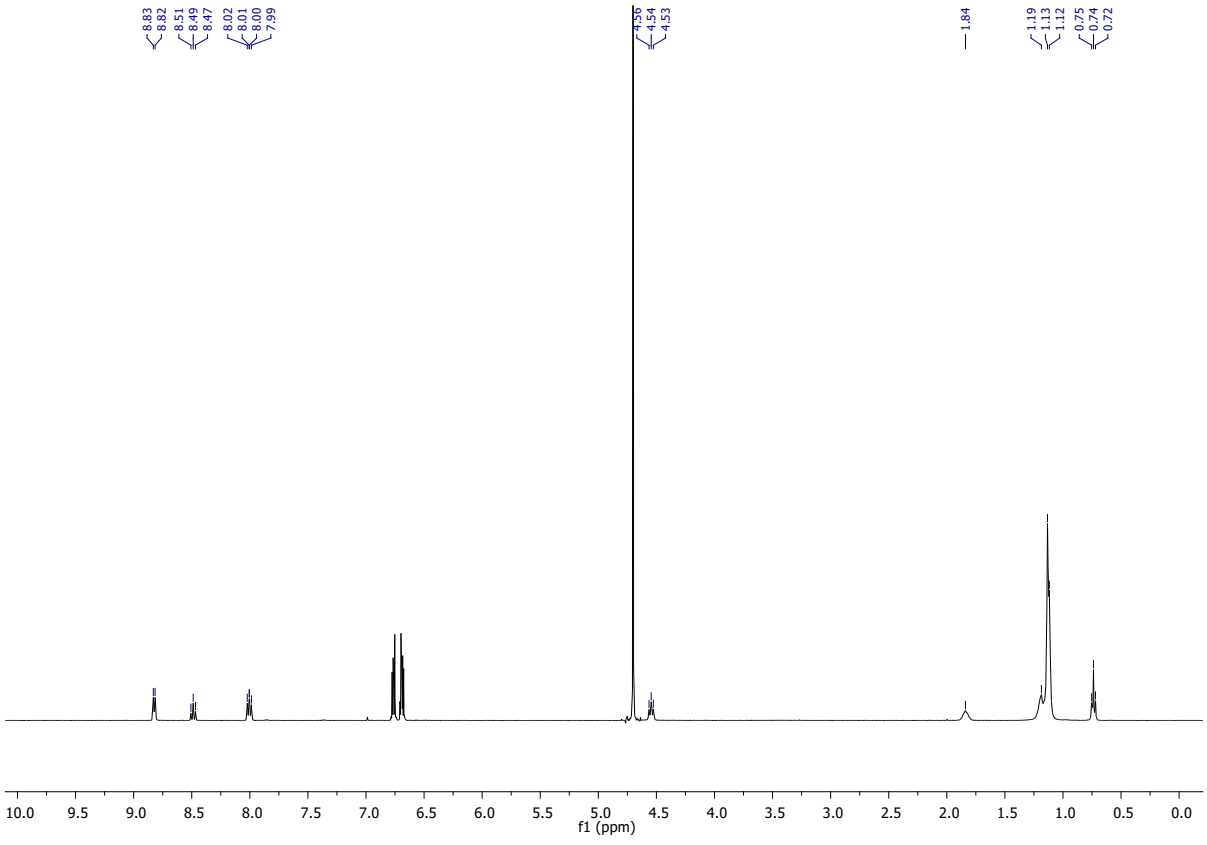

$^{1}$H NMR of CPB & 0.08M 1,2-diaminobenzene

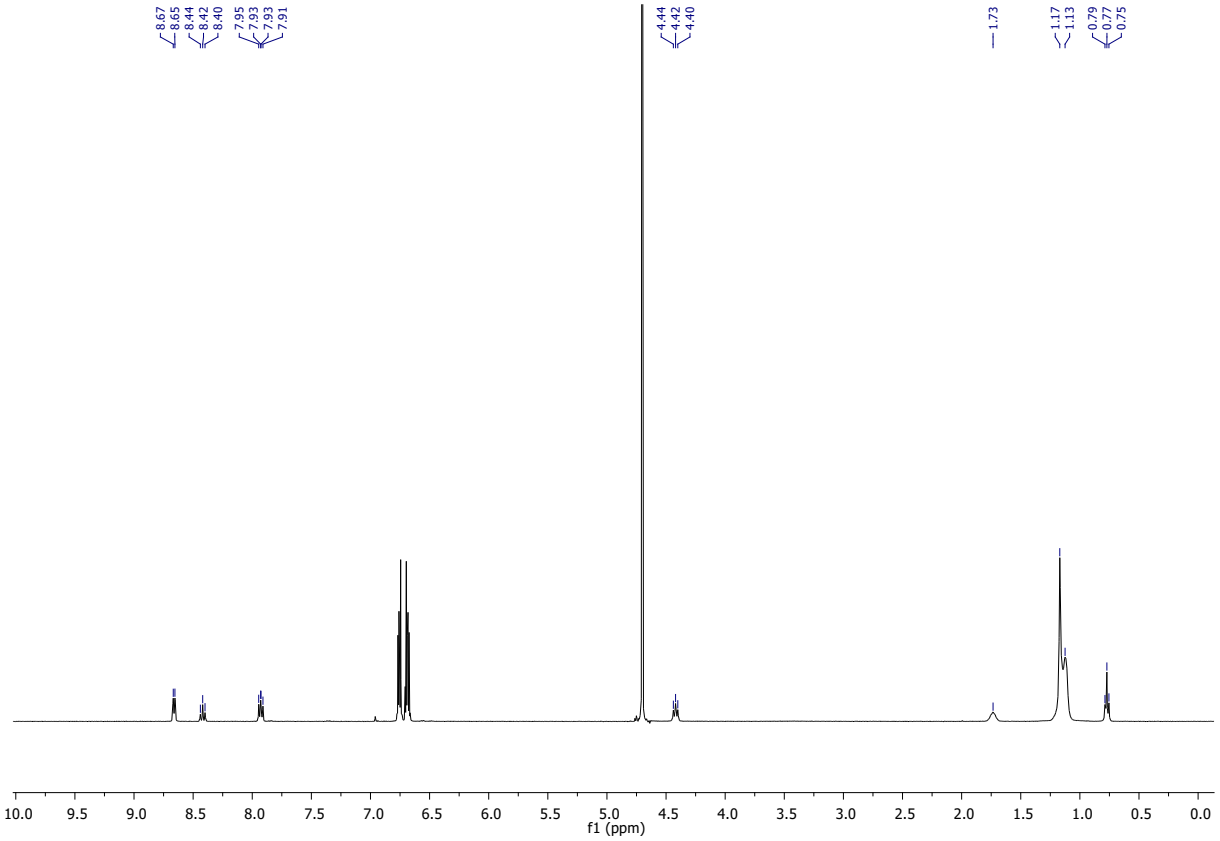


$^{1}$H NMR of CPB & 0.16M 1,2-diaminobenzene

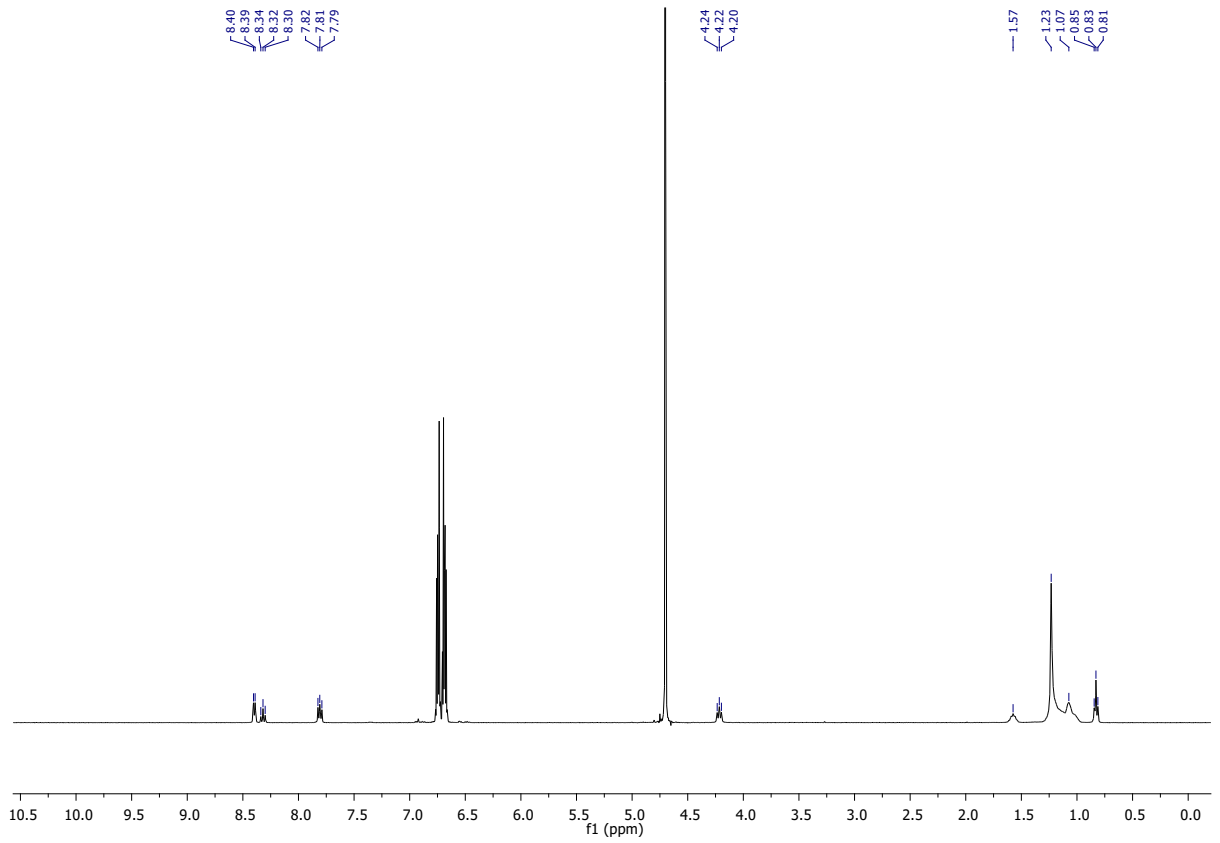

$^{1}$H NMR of CPB & 0.32M 1,2-diaminobenzene

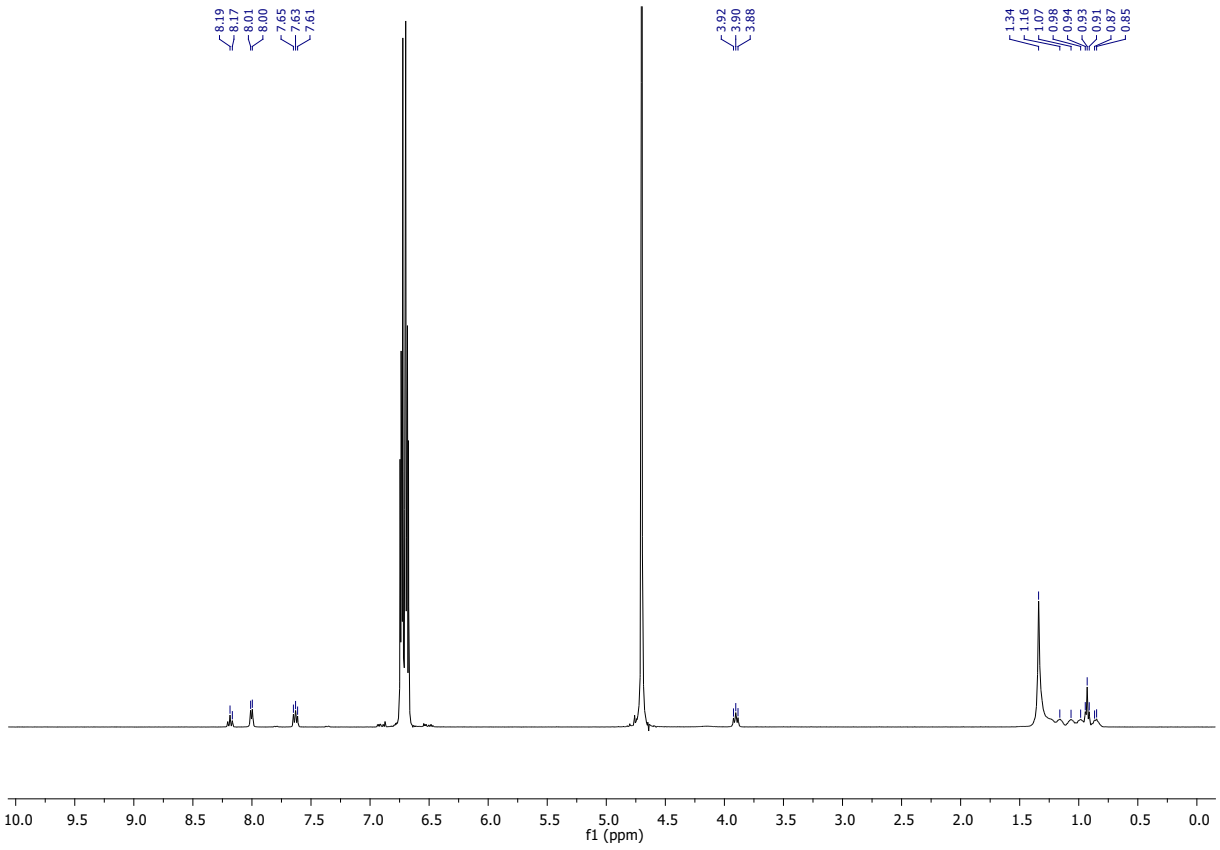

$^1$H NMR of CPB & 0.02M styrene

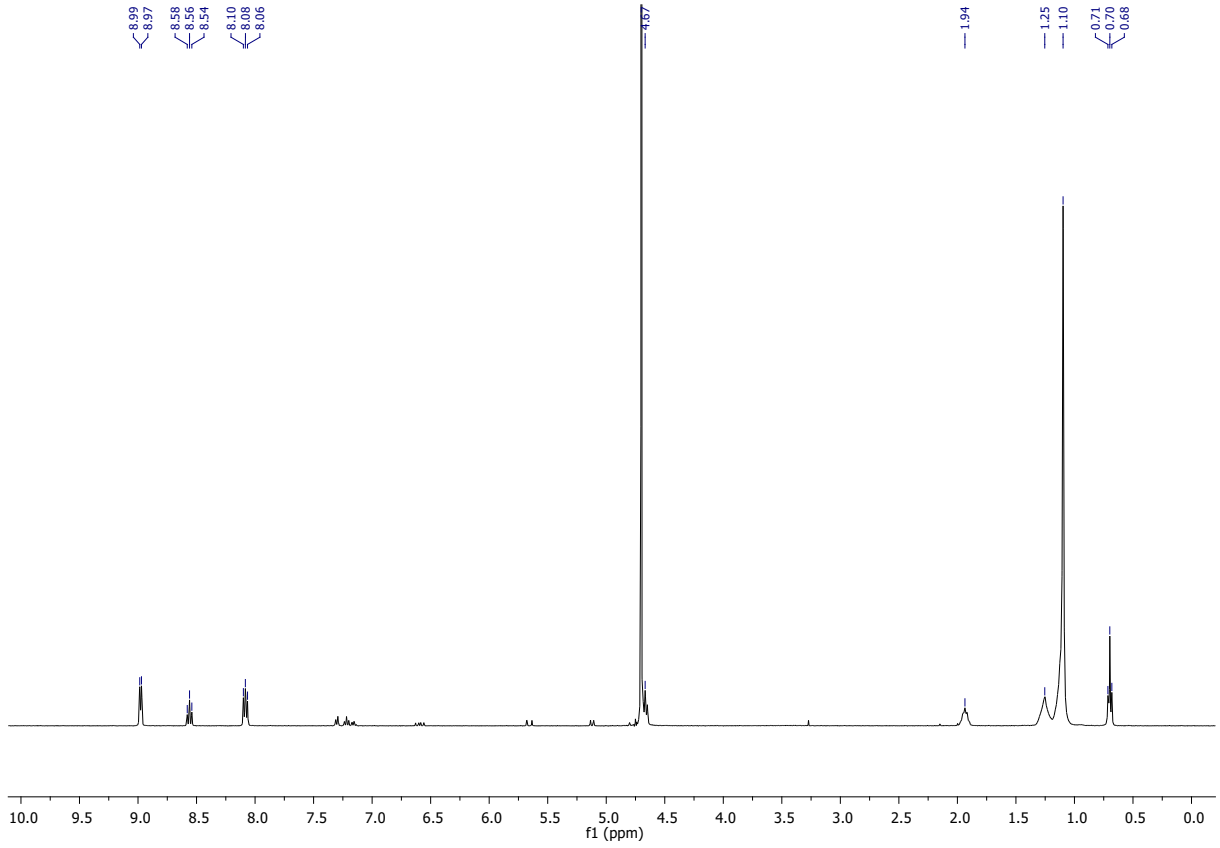


$^1$H NMR of CPB & 0.04M styrene

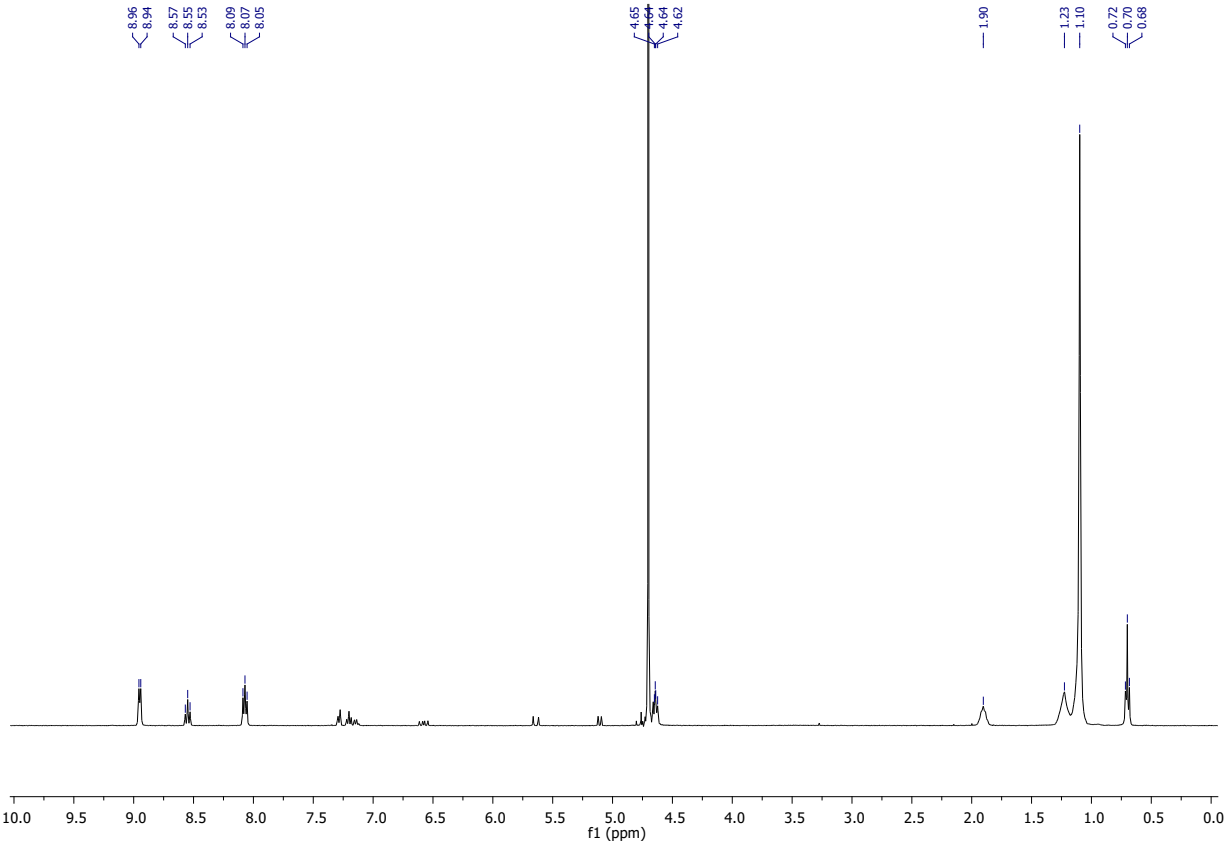

$^1$H NMR of CPB & 0.08M styrene

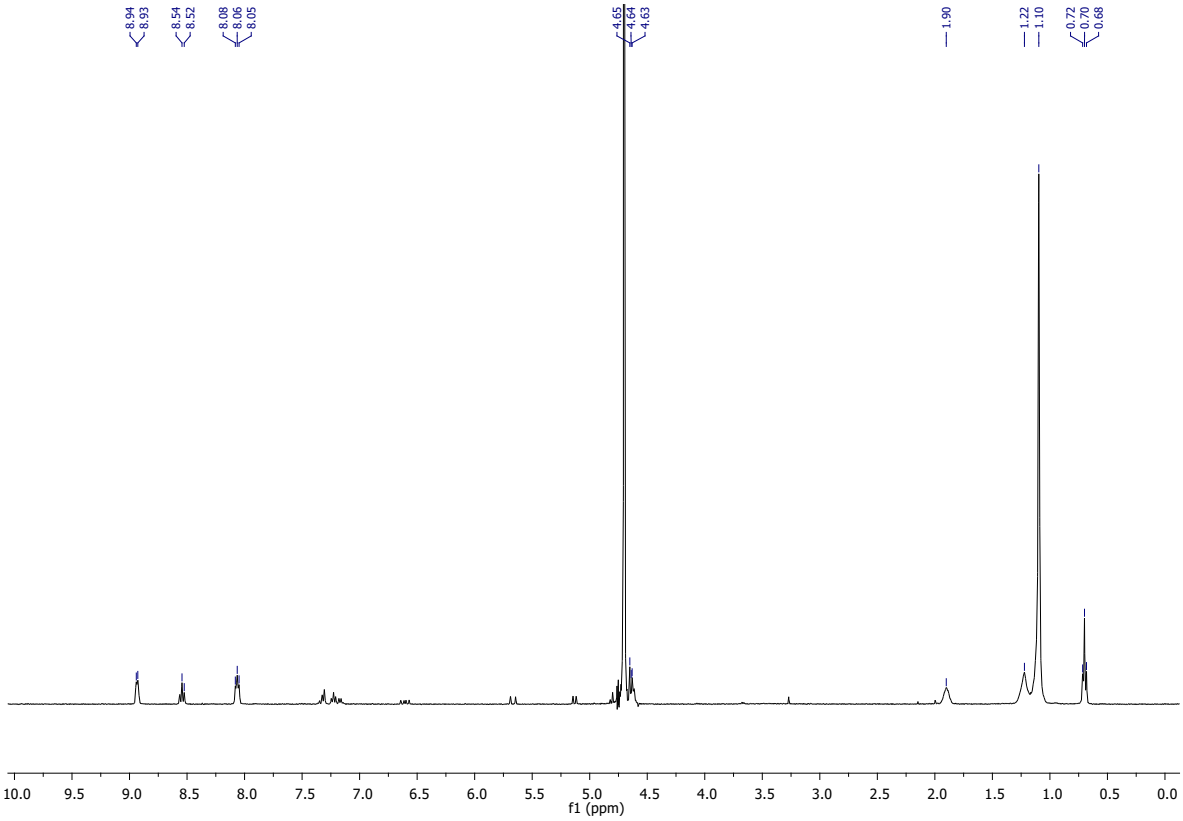


$^1$H NMR of CPB & 0.16M styrene

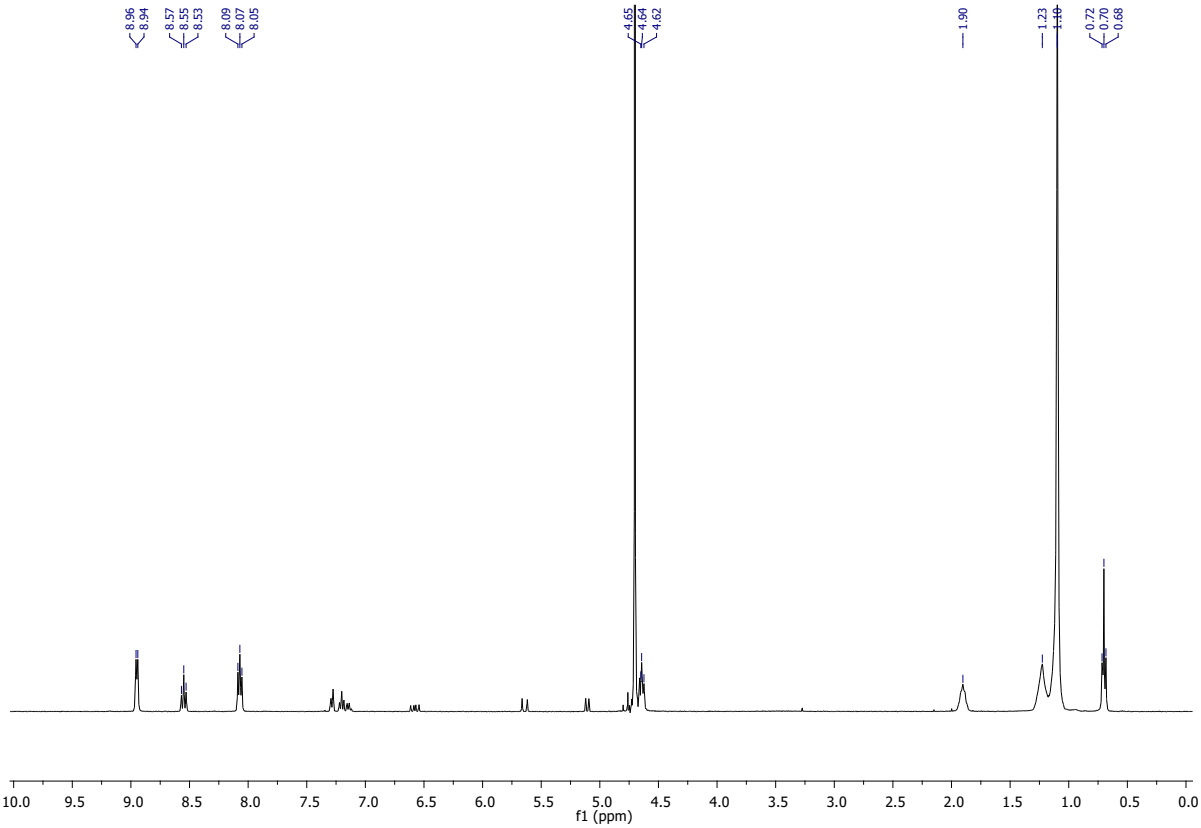

$^1$H NMR of CPB & 0.32M styrene

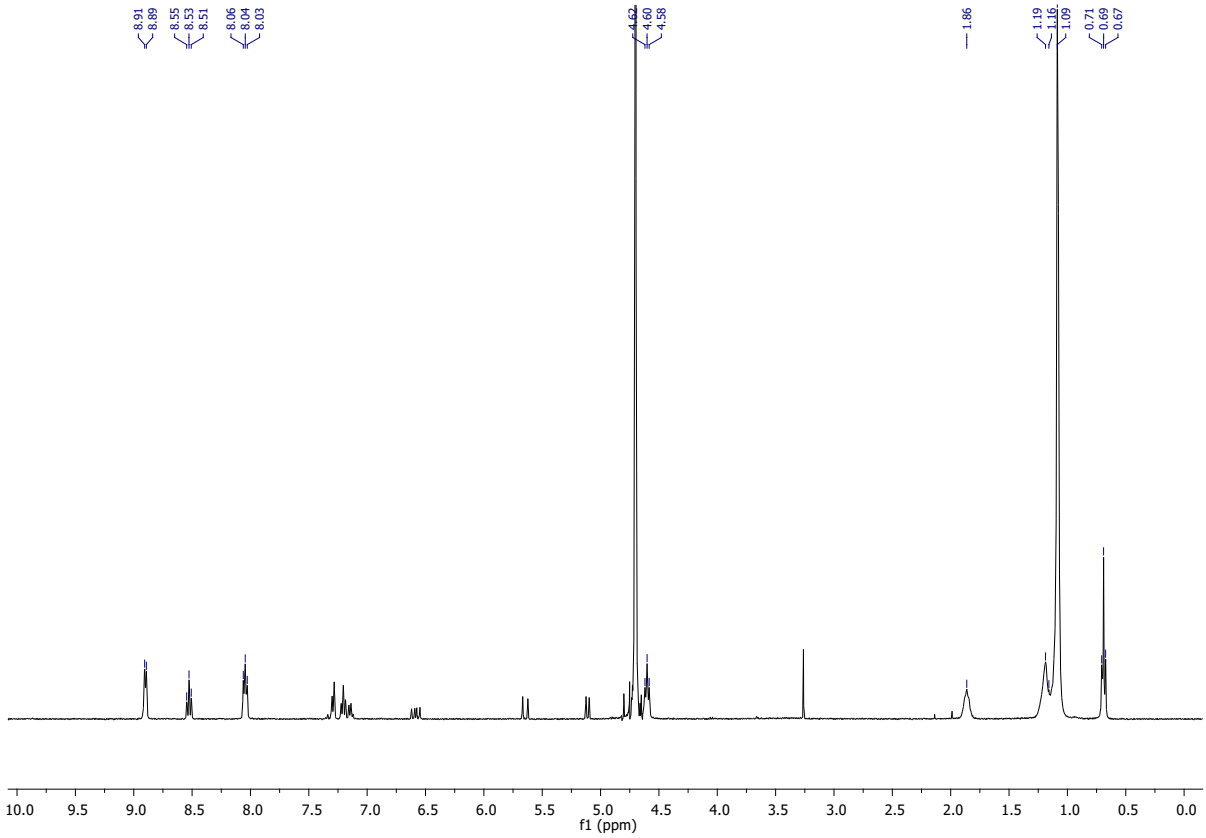


## Theoretical calculations

**Table S3.** Gibbs free energy changes (ΔG) and binding energy (ΔE) of **1a_CPB** and **2a_CPB** using optimized geometries at B3LYP/3-21G* level of theory in aqueous phase.(BSSE corrected).

| Complex | Gibbs free energy changes (ΔG) (Kcal/mol) | Binding energy (ΔE) (Kcal/mol) |
|---|---|---|
| **1a_CPB** | -2.493 | -12.134 |
| **2a_CPB** | -7.347 | -17.883 |

**Table S4.** Calculated HOMO-LUMO gaps.

| Molecule | $E_{HOMO}$ (a.u) | $E_{LUMO}$(a.u) | $E_{gap}$ (a.u) |
|---|---|---|---|
| **1a** | -0.35492 | -0.20851 | 0.14641 |
| **2a** | -0.30313 | -0.16430 | 0.13883 |
| **CPB** | -0.37641 | -0.19511 | 0.18130 |
| **1a_CPB** | -0.35577 | -0.21078 | 0.14499 |
| **2a_CPB** | -0.30227 | -0.19795 | 0.10432 |

**Table S5**: The calculated topological parameters (in au) to predict and determine the nature of non-covalent interaction (NCI).

| Complex | Interaction | number | total electron density | laplacian of electron density | V(r) | G(r) | K(r) | V(r)/G(r) |
|---|---|---|---|---|---|---|---|---|
| **1a_CPB** | 3, +1 | 84 | 0.0225278737 | 0.1424549786 | -0.025846990 | 0.030730367 | -0.004883376 | -0.841089532 |
| | 3, +1 | 104 | 0.0037408284 | 0.0141180608 | -0.002241696 | 0.002885605 | -0.000643909 | -0.776854767 |
| | 3, +1 | 114 | 0.0042846456 | 0.0166565515 | -0.002301953 | 0.003233045 | -0.000931092 | -0.818412536 |
| | 3, +1 | 121 | 0.0028553423 | 0.0105537498 | -0.001404367 | 0.002021402 | 0.000617035 | -0.694748991 |
| | 3, +1 | 141 | 0.0216209542 | 0.1305345258 | -0.022889611 | 0.027761621 | -0.004872010 | 0.824505564 |
| **2a_CPB** | 3, +1 | 114 | 0.0225586015 | 0.1422131987 | -0.025901626 | 0.3072746331 | -0.004825836 | -0.084294709 |
| | 3, +1 | 137 | 0.0025356700 | 0.010572507 | -0.001323726 | 0.001983426 | -0.000659700 | -0.667393691 |
| | 3, +1 | 141 | 0.0072242983 | 0.026100948 | -0.005073754 | 0.005799495 | -0.000725741 | -0.874861345 |
| | 3, +1 | 149 | 0.0211206850 | 0.127090554 | -0.022102394 | 0.026937516 | -0.004835122 | -0.819360997 |

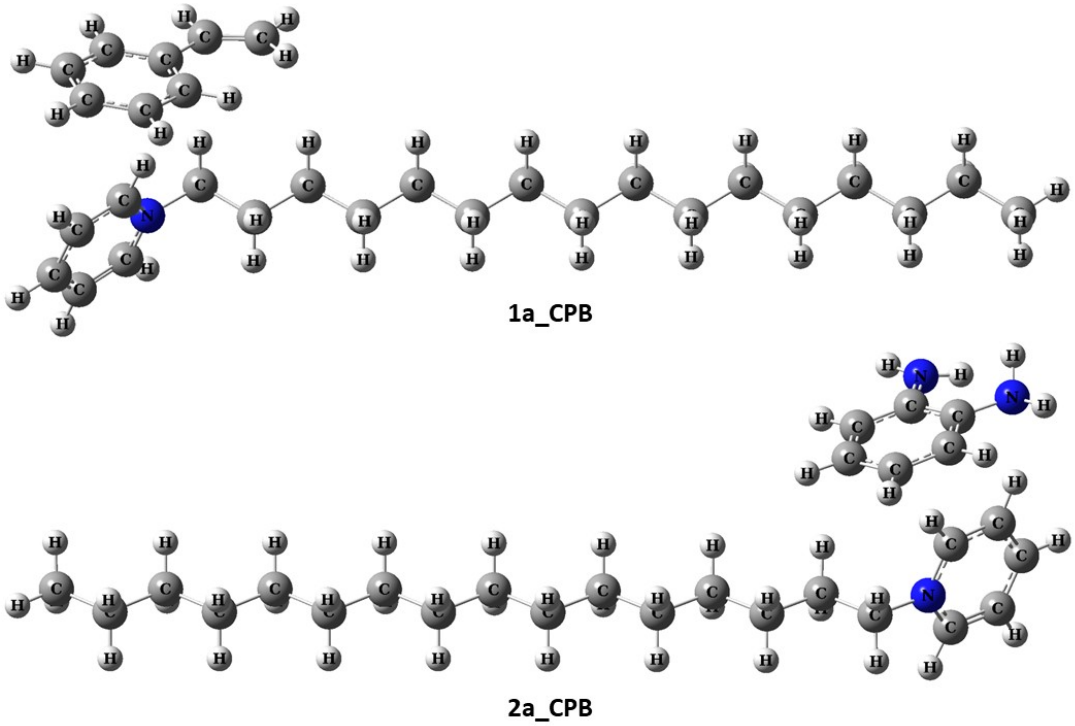


**Figure S3**: Ground state ($S_0$) optimized structures of **1a_CPB** and **2a_CPB** complexes at B3LYP/3-21G* level of theory in aqueous phase.

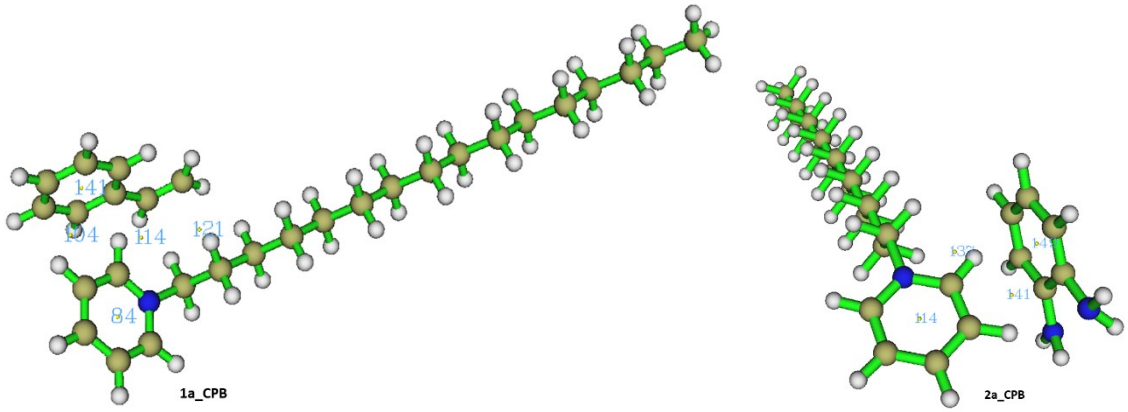


**Figure S4**: Critical points (3,+1) of **1a_CPB** and **2a_CPB** in aqueous phase.

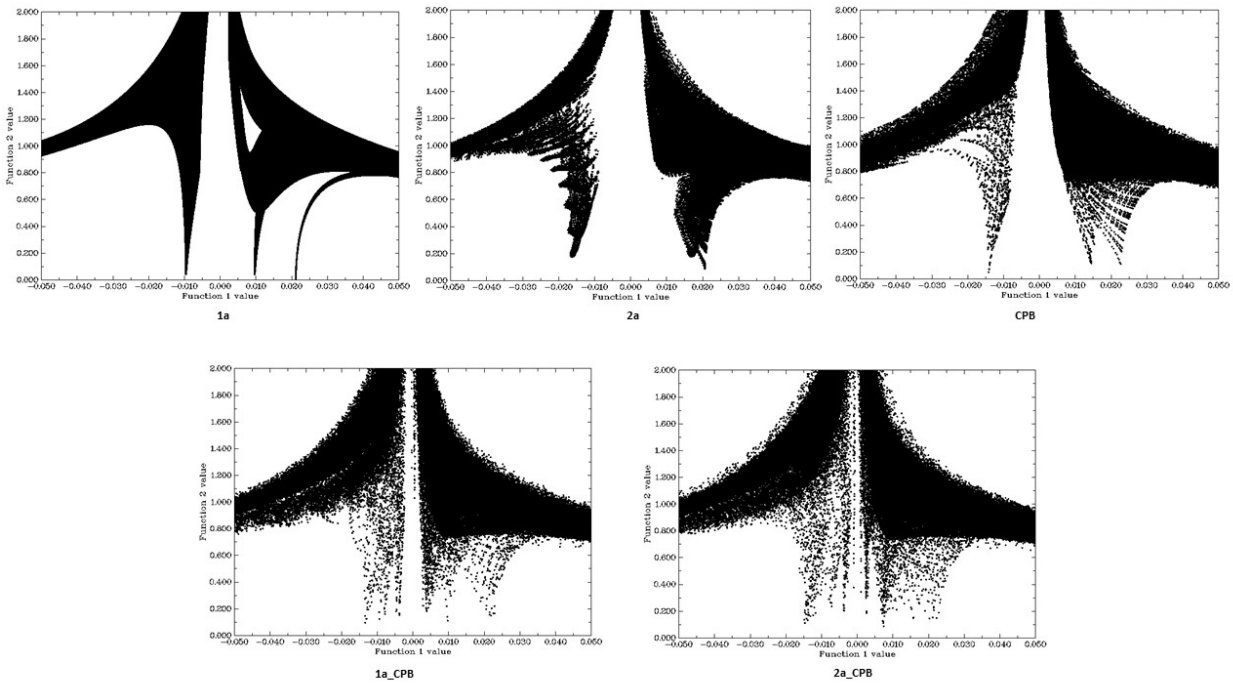


**Figure S5**: NCI scatter graphs of **1a**, **2a**, **CPB**, **1a_CPB** and **2a_CPB** in aqueous phase. {Function 1 denote sign($\lambda_2$)*ρ where $\lambda_2$ is the second largest eigen value of Hessian matrix of electron density and ρ is electron density in corresponding region; and function 2 represent reduced density gradient (RDG)}.